ELEMENTA
Science of the Anthropocene

Weger, LB, et al. 2019. Modeling the impact of a potential shale gas industry in Germany and the United Kingdom on ozone with WRF-Chem. *Elem Sci Anth,* 7: 49. DOI: https://doi.org/10.1525/elementa.387

RESEARCH ARTICLE

Modeling the impact of a potential shale gas industry in Germany and the United Kingdom on ozone with WRF-Chem

Lindsey B. Weger*,†, Aurelia Lupascu*, Lorenzo Cremonese* and Tim Butler*,‡

Germany and the United Kingdom have domestic shale gas reserves which they may exploit in the future to complement their national energy strategies. However gas production releases volatile organic compounds (VOC) and nitrogen oxides (NO_x), which through photochemical reaction form ground-level ozone, an air pollutant that can trigger adverse health effects e.g. on the respiratory system. This study explores the range of impacts of a potential shale gas industry in these two countries on local and regional ambient ozone. To this end, comprehensive emission scenarios are used as the basis for input to an online-coupled regional chemistry transport model (WRF-Chem). Here we simulate shale gas scenarios over summer (June, July, August) 2011, exploring the effects of varying VOC emissions, gas speciation, and concentration of NO_x emissions over space and time, on ozone formation. An evaluation of the model setup is performed, which exhibited the model's ability to predict surface meteorological and chemical variables well compared with observations, and consistent with other studies. When different shale gas scenarios were employed, the results show a peak increase in maximum daily 8-hour average ozone from 3.7 to 28.3 μg m^{-3}. In addition, we find that shale gas emissions can force ozone exceedances at a considerable percentage of regulatory measurement stations locally (up to 21% in Germany and 35% in the United Kingdom) and in distant countries through long-range transport, and increase the cumulative health-related metric SOMO35 (maximum percent increase of ~28%) throughout the region. Findings indicate that VOC emissions are important for ozone enhancement, and to a lesser extent NO_x, meaning that VOC regulation for a future European shale gas industry will be of especial importance to mitigate unfavorable health outcomes. Overall our findings demonstrate that shale gas production in Europe can worsen ozone air quality on both the local and regional scales.

Keywords: Shale gas; WRF-Chem; European air quality; Ozone; Methane leakage; Emission scenarios

Introduction

Natural gas production in the United States (US) has risen markedly over the past years: in 2018, US dry gas production was 30 trillion cubic feet (861 billion cubic meters; bcm), an increase of 69% over 2005 levels (EIA, 2019a). The majority of the US gas production increase since 2005 was afforded through shale resources (EIA, 2016). In fact, shale gas made up approximately 69% of total US natural gas production in the year 2018 (EIA, 2018). Commercial extraction of shale gas reservoirs has been made possible through relatively recent advancements in horizontal drilling and hydraulic fracturing technologies. While shale gas production has hitherto largely been an American phenomenon (BP, 2016), global shale gas resources[1] are vast totaling more than 200 trillion cubic meters (tcm; about one third of world total gas technically recoverable resources), with about 13 tcm in Europe (EIA, 2013). Though there is currently no European commercial shale gas industry, several countries there have considered using domestic supplies to complement their national energy strategy (EC, 2014; JRC, 2012). Shale gas has the potential to reduce dependency on foreign imports and to offset the decline in indigenous production of conventional gas that European countries have been experiencing (BP, 2017). While Poland was initially a promising location for commercial shale gas extraction, exploration efforts there ultimately failed (LaBelle, 2018). On the other hand, Germany and the United Kingdom (UK) have among the top European shale gas-in-place[2] volumes (Germany: 7.7 tcm; UK: 37.6 tcm), and have expressed interest in recent years in exploiting their reserves (BGR, 2016; BGS, 2013). Additionally many reports and papers

* Institute for Advanced Sustainability Studies (IASS), Potsdam, DE
† Institut für Geowissenschaften, Universität Potsdam, Potsdam, DE
‡ Institut für Meteorologie, Freie Universität Berlin, Berlin, DE
Corresponding author: Lindsey B. Weger (lindsey.weger@iass-potsdam.de)

have been published on European shale gas and for the UK and Germany in particular, e.g., ACATECH (2016), AQEG (2018), BGR (2012), Broomfield et al. (2014); Cotton et al. (2014), DECC (2013), DECC (2014), Hays et al. (2015), McGlade et al. (2014), MULNV NRW (2012), Pfunt (2016), Sauter et al. (2013), SGD (2013), Society (2012) SRU (2013), Stamford and Azapagic (2014), UBA (2013, 2014).

Methane (CH_4) is the main constituent of natural gas, and is leaked throughout the various stages of production. CH_4 is a potent greenhouse gas with a heat-trapping ability 87 times that of CO_2 over a 20-year time frame, or 36 over a 100-year time frame (Myhre et al., 2013). Accordingly numerous studies have focused in recent years on CH_4 loss from natural gas production, reporting CH_4 leakage rates[3] ranging from less than 1% to greater than 10% of natural gas production, e.g., Allen et al. (2013), Alvarez et al. (2018), Caulton et al. (2014), Howarth (2014), Karion et al. (2013), Peischl et al. (2015, 2013), Pétron et al. (2012, 2014), Schneising et al. (2014). Findings from studies suggest that oil and gas sector CH_4 emissions are higher than official inventory estimates, with superemitters likely responsible for a large fraction of the CH_4 leakage (Brandt et al., 2014; Johnson et al., 2017; Miller et al., 2013; Zavala-Araiza et al., 2015). For example Alvarez et al. (2018) estimated a CH_4 leakage rate of 2.3% for about one third of US gas production and distribution systems, roughly 60% higher than the US EPA inventory estimate. To put these values into perspective, Alvarez et al. (2012) found that a CH_4 leakage rate of 3.2% or greater would negate climate benefits gained by switching from coal to natural gas power plants. In addition, toxic pollutants are likewise released, including volatile organic compounds (VOCs), nitrogen oxides (NO_x), particulate matter (PM), and carbon monoxide (CO), e.g., Roy et al. (2014), Schade and Roest (2016).

In the presence of sunlight, VOCs, CH_4, and CO interact with NO_x through a complex series of reactions to form tropospheric ozone (O_3) (Sillman, 1999; Sillman, 2003). The relationship between O_3 and its precursors is nonlinear: in a NO_x-sensitive regime (high VOC/NO_x ratio), O_3 increases with increasing NO_x, while increasing VOCs will have little to no impact. In a VOC-sensitive regime (low VOC/NO_x ratio), O_3 increases with increasing VOCs, while the addition of NO_x decreases O_3 formation. VOC-sensitive regimes are often encountered in urban areas where emissions of NO_x from combustion (e.g., in road traffic) are high, while NO_x-sensitive cases are often found in rural areas.

Ground-level O_3 is a significant short-lived climate forcer (Myhre et al., 2013), and dangerous to human and environmental health (Amann et al., 2008). O_3 adversely affects the respiratory, cardiovascular and central nervous systems, reproduction and development (EPA, 2013; Horvath and McKee, 1993; Nuvolone et al., 2018), damages ecosystems (EPA, 2013; Horvath and McKee, 1993; Nuvolone et al., 2018), reduces crop yields (Avnery et al., 2011), and impairs infrastructure (Kumar and Imam, 2013; Lee et al., 1996). The European Union's (EU) air quality directive asserts that the maximum daily 8-hour average O_3 (MDA8) should not surpass 120 $\mu g\ m^{-3}$ (60 ppb[4]) as a long-term objective; as a target value it should not be exceeded on more than 25 days per year averaged over 3 years (EP, 2002). However, the EU's target value for O_3 is higher than the World Health Organization's (WHO) air quality guideline of 100 $\mu g\ m^{-3}$, which they recommend to adequately protect public health (WHO, 2005). In spite of extensive regulation of precursor emissions, O_3 pollution is still a problem in Europe: according to the European Environmental Agency (EEA), over the 2000–2015 period between 94–99% of the European urban population (EU-28) was exposed to O_3 levels exceeding the WHO guideline (EEA, 2017). Exposure to O_3 pollution is believed to cause thousands of premature deaths of Europeans annually, with 13,600 deaths estimated for 2014 (EU-28) (EEA, 2017). Unhealthy levels of ambient O_3 in Europe can be ascribed to rising hemispheric background O_3 (Monks et al., 2015), the transboundary nature of O_3 and its precursors i.e. they can be transported across national boundaries and regions (Bach et al., 2014), reduced NO_x titration in some urban areas whereby O_3 is scavenged through reaction with NO (Amann et al., 2008), and the nonlinear relationship between O_3 and its precursors (EEA, 2014).

Atmospheric chemistry transport modeling is a valuable tool for assessing air quality on the local and regional levels and assisting in air quality management. A widely used model is the regional scale air quality WRF-Chem model (Grell et al., 2004). WRF-Chem has frequently been used in European-based air quality studies in recent years, e.g., Brunner et al. (2015), Fallmann et al. (2016), Forkel et al. (2012), Im et al. (2015), Kuik et al. (2016, 2018), Mar et al. (2016), Solazzo et al. (2012a, 2012b), Tuccella et al. (2012), Zhang et al. (2013a, 2013b), among others.

Intensive natural gas production has motivated several modeling studies to assess the role of precursor emissions from this source in regional O_3 formation. Rodriguez et al. (2009) found that increased growth in oil and gas activities in the US Intermountain West could increase MDA8 by a maximum of 9.6 ppb in southwestern Colorado and northwestern New Mexico in the summertime. Kemball-Cook et al. (2010) modeled the impact of shale gas development in the Haynesville Shale play for 2012 and found increases in MDA8 up to 5 ppb within Northeast Texas and Northwest Louisiana. Carter and Seinfeld (2012) looked at the relative contributions of NO_x, individual VOCs and HONO (nitrous acid) in O_3 formation during episodes in the wintertime in the gas producing Upper Green River Basin region in Wyoming; they found that the locations varied in their sensitivity to VOC and NO_x emissions: one site for the 2008 episode was highly NO_x sensitive, while the other 2008 site and both sites for 2011 were highly VOC sensitive. Ahmadov et al. (2015) simulated high O_3 episodes during the winter of 2013 over the intensive oil and gas producing Uinta Basin in the Western US, finding that a simulation based on top-down oil and gas sector emissions was able to capture observations during high O_3 episodes, while a simulation using bottom-up emissions from the US Environmental Protection Agency's (EPA) National Emission Inventory did not. Fann et al. (2018) modeled the impact of oil and gas activities over the US for 2025, predicting increases in summertime MDA8 up

to 8.12 ppb in Western Texas. Archibald et al. (2018) modeled over the UK the potential impacts of VOC and NO_x emissions related to future shale gas fracking activities there for 2013 and generally found increases in MDA8 across the country throughout the year with a maximum increase of 2.3 ppb in June. In addition to these studies, much of the literature on US shale gas has focused on O_3, e.g., AACOG Natural Resources Department (2013, 2015), Chang et al. (2016), Edwards et al. (2014), Field et al. (2015), Helmig et al. (2014), Koss et al. (2015), NC Division of Air Quality (2015), Olaguer (2012), Schade (2017), Schnell et al. (2009). These works underline the value and need for studies that analyze how O_3 may be affected by oil and gas development.

Shale gas is a contentious topic among the public and political spheres in both Germany and the UK, with critics citing various concerns, e.g., adverse air quality impacts (Althaus, 2014; Cremonese et al., 2015; Vetter, 2016; Yeo, 2019). The German government currently has a moratorium on unconventional fracking activities, e.g. for shale, which can be reevaluated in 2021 (German Federal Government, 2017). On the other hand, the British government recently granted consent for hydraulic fracturing testing to the energy company Cuadrilla in late 2018 (Perry, 2018). However, the UK's safety regulations strictly limit the magnitude of seismic activity allowed by fracking activities, currently set to 0.5 on the Richter scale, which severely constrains the amount of gas that can be extracted (Thomas and Pickard, 2019). Indeed, tremors exceeding this limit have forced Cuadrilla to suspend work on numerous occasions since testing started. In any case, what role shale gas production will have in Europe's future, if any, is uncertain. In order to inform decisions and the greater debate on shale gas, scientifically-based knowledge on potentially dangerous impacts is critical. To this end, air quality modeling can be used to run scenarios and study how varying levels of precursor emissions from a future shale gas sector may impact regional European O_3 pollution.

This paper is a companion paper to Cremonese et al. (2019), who developed scenarios on a future shale gas industry in these two countries to quantify the potential impacts on greenhouse gas and pollutant emissions. The present study builds on Cremonese et al. (2019) by using their scenario work as the basis for emissions input to the WRF-Chem model to investigate the range of potential impacts from shale gas on local and regional O_3, with a major focus on O_3 health-related metrics MDA8 and SOMO35 (annual Sum of Ozone Means Over 35 ppb, daily maximum 8-hour). In addition to the CH_4 leakage rate of Cremonese et al. (2019), we also investigate higher CH_4 leakage rates from other studies up to 6%. Due to our interest in the European region, we base our WRF-Chem setup on Mar et al. (2016), whose evaluated setup over Europe performed well for both meteorology and chemistry. Our objective is to improve understanding on potential air quality impacts from a future shale gas industry in Europe for public and political discourse, and for supporting policymakers and other decision-makers. Further our work can inform regulation of a potentially emerging industry to enact emission control strategies and prevent potentially harmful levels of air pollution. To our knowledge, there have been no published studies of regional air quality impacts from future shale gas activities in Europe, apart from Archibald et al. (2018), which focused on the UK. In this paper, we first describe the methodology, detailing the model setup, initial and boundary conditions and emissions input, the shale gas scenarios, and the preprocessing of shale gas emissions. Subsequently we discuss the results, and finish with a summary and conclusions.

Methodology

Model description and emissions

We used the Weather Research and Forecasting model (WRF) version 3.8.1 (Skamarock et al., 2008), coupled with chemistry (WRF-Chem) (Fast et al., 2006; Grell et al., 2005). Additionally we employ the same principal WRF-Chem options as done by Mar et al. (2016), who performed an extensive evaluation over Europe for the entire year of 2007 with WRF-Chem version 3.5.1. Here we describe our setup, and the main options we use are summarized in **Table 1**. The namelist is provided in SM Text S1, Table S1.

The model domain is set over Western Europe and fully covers the countries of study (i.e., Germany and the

Table 1: Options used in WRF-Chem model simulations. DOI: https://doi.org/10.1525/elementa.387.t1

Atmospheric process	Option used
Cloud microphysics	Lin et al. scheme (Lin et al., 1983)
Longwave radiation	RRTMG (Iacono et al., 2008)
Shortwave radiation	Goddard shortwave scheme (Chou and Suarez, 1994)
Surface layer	MM5 Monin-Obukhov scheme (Jiménez et al., 2012)
Land-surface physics	Noah land surface model (Chen and Dudhia, 2001)
Urban surface physics	Urban canopy model (Kusaka and Kimura, 2004)
Planetary boundary layer	Yonsei University scheme (Hong et al., 2006)
Cumulus parameterization	Grell 3D scheme (Grell and Dévényi, 2002)
Chemistry	MOZART-4 chemistry, KPP solver
Photolysis	Madronich F-TUV photolysis

UK; **Figure 1**). The horizontal grid resolution was set to 15 km × 15 km, and the model domain was established with 150 grid points in both the west–east and south–north directions. We used 35 vertically-stretched levels in the model with the top layer at 50 hPa. Our simulation period spans from May 29, 2011 to September 1, 2011, where the days in May serve as model spin-up. We decided on JJA (June, July, August) as the period for which to run our simulations because meteorological conditions during the summer months, i.e., elevated temperatures, increased sunlight and slow-moving high pressure systems, are more favorable to production of high and potentially harmful levels of tropospheric O_3, and therefore this season commonly experiences adverse impacts on and air quality in terms of this pollutant, e.g., EEA (2017), Volz-Thomas and Ridley (1994).

Meteorological initial and lateral boundary conditions (BCs) were obtained from the ERA-Interim reanalysis dataset provided by the European Centre for Medium-range Weather Forecast (ECMWF; Dee et al., 2011) with a spatial resolution of ~80 km every 6 hours. We used nudging by four dimensional data assimilation (FDDA) to reduce model errors in meteorology that may be associated with deviation of simulated large-scale circulation from the observed synoptic conditions. We nudged temperature at all vertical levels, while horizontal winds are nudged above the planetary boundary layer (PBL). Mar et al. (2016) reported erroneous precipitation suppression over Europe in sensitivity studies compared with observations when water vapor nudging was applied; therefore we likewise did not nudge water vapor in our simulations, also following the approach of, e.g., Miguez-Macho et al. (2004) and Stegehuis et al. (2015). Space- and time-varying (i.e., dynamic) chemical initial and lateral BCs were implemented in this study and were provided by simulations from MOZART-4/GEOS-5 through NCAR at http://www.acom.ucar.edu/wrf-chem/mozart.shtml. Note that dynamic BC data can improve simulated O_3 (Gavidia-Calderón et al., 2018), and MOZART-4 global model data is frequently used as the BCs for simulations (Pfister et al., 2011).

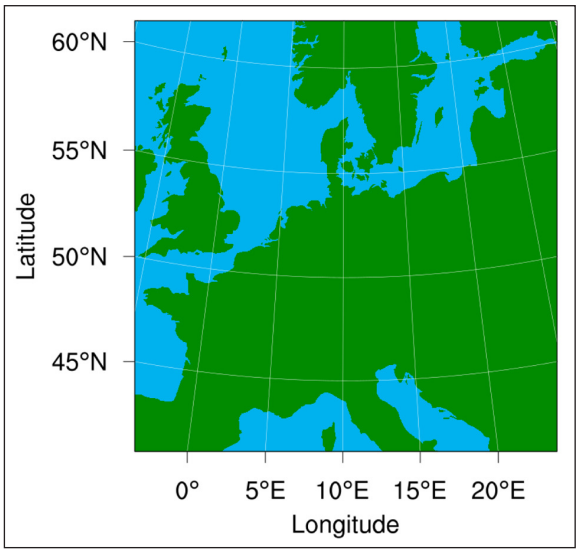

Figure 1: Domain of study. Model domain applied in WRF-Chem simulations, set over Western Europe and fully covering the countries under examination, Germany and the UK. DOI: https://doi.org/10.1525/elementa.387.f1

Based on the findings of Mar et al. (2016), we apply the MOZART-4 chemical mechanism in our simulations (Emmons et al., 2010). Of the natural gas-relevant VOC species that are considered in this work, ethane and propane are represented explicitly by the MOZART-4 mechanism, while the higher alkanes (i.e., butane, pentane, hexane and heptane) are lumped into the C > 3 group known as BIGALK. Note that VOC shale gas emissions in this study are very light and do not contain aromatics (**Table 4**), and NO_x emissions are likewise low compared with national inventories (**Figure 3**). This means that their effect on secondary aerosol formation would likely be insignificant, and as such we do not look at this in our study. Anthropogenic emissions of CO, NO_x, SO_2, VOCs, and NH_3 used in WRF-Chem were obtained from the TNO MACC III inventory provided at a resolution of 7 km × 7 km, for the year 2011 (Kuenen et al., 2014). In addition to the aforementioned anthropogenic emissions, shale gas emissions based on Cremonese et al. (2019) were included in our simulations (described in Scenario background).

Shale gas emission scenarios

Scenario background

The present study carries on the work of Cremonese et al. (2019), who developed a series of drilling and emission scenarios to study the effects of a potential shale gas industry in Europe on greenhouse gas and pollutant release. Specifically, they explore inter alia how different practices, uncertainty in data – i.e., activity data and emission factors, as well as the extent of well productivity, may impact emissions released annually from such an industry in Europe. The scope of Cremonese et al. (2019)'s scenarios covers upstream emissions, i.e., from well pad preparation up to gas processing, from shale gas development in Germany and the UK. Cremonese et al. (2019) assume in their scenarios that annual shale gas production will be equivalent to recent conventional production in these two countries (Germany: 11.6 bcm; UK: 36.6 bcm). All scenarios explored in the present study are based on the 'REm-U P25' scenario in Cremonese et al. (2019). REm stands for – 'Realistic Emissions' case, meaning that business as usual practices for US shale gas production are applied; -U stands for 'Upper' meaning that activity data and emission factors are on the high end of the uncertainty range. P25 means that well productivity is at the 25th percentile, i.e., the lower end of the spectrum of well productivity as determined by the authors. CH_4 leakage rates from REm-H P25 are up to 1.36%, which are well within the range predicted for average upstream natural gas leakage in the US and worldwide (Cremonese et al,. 2019). While European official CH_4 leakage estimates for natural gas systems are, comparatively, substantially lower, independent studies investigating European natural gas CH_4 leakage rates in a transparent way are unavailable (Cremonese et al. (2019) and references therein). Indeed recent studies suggest

that CH_4 emissions from European oil and gas systems are higher than indicated by inventories (Riddick et al., 2019; Yacovitch et al., 2018), while numerous studies carried out in the US have reported emissions from natural gas systems which are higher than national estimates (Introduction). Hence it is reasonable to explore higher leakages as unanticipated, yet plausible rates for large-scale gas production in Europe.

Present work

In total, we examine three scenario sets covering low, medium and high shale gas emissions which we refer to respectively as SG1, SG2, and SG3. Our interest is to see how varying emissions of VOCs with constant NO_x from shale gas activities may affect air quality in this region. Note that the shale gas emissions from Cremonese et al. (2019) included in our scenarios are NO_x, CO and VOCs. NO_x and CO are based on combustion processes, while VOC emissions are based on CH_4 leakage as the two species are co-emitted together in gas leaks. Due to its relevance to the literature on natural gas, we explore scenarios based on varying CH_4 leakage rates. Therefore NO_x and CO shale gas emissions remain constant in SG1-3, while VOC emissions (based on extent of CH_4 leakage) are the only ones that vary between the three scenario sets. It is necessary to note that changes in the CH_4 emissions are not used in this study due to model limitations as will be explained in Pre-processing shale gas emissions for WRF-Chem. In SG1 we use the CH_4 leakage rates directly from Cremonese et al. (2019), which are tailored specifically to Europe (**Table 2**). For SG2 medium level emissions, we chose a rate of 2% based on Alvarez et al. (2018) (the approximate value for the segment of the gas chain considered in our scenarios), as it is relatively high yet still representative of large-scale gas production in the US (Introduction). For SG3 high level emissions, we chose a conservative extreme value of 6% which is on the higher end of the literature for CH_4 leakage (typically ranging from <1.0 to 10%, e.g., Visschedijk et al., 2018). As reported in Saunois et al. (2016), the GAINS model adopted a CH_4 emission factor of 4.5% for shale gas mining with current technology, which also supports our choice of 6% as a conservative extreme rate.

Within each scenario set we explore three "sub" scenarios resulting in a total of nine simulated emission scenarios (**Table 2**), in addition to a baseline scenario for comparison. These three scenarios are wet gas composition, dry gas composition, and concentrated NO_x emissions, which we abbreviate to 'wet gas', 'dry gas', and 'conNO_x'. The first two are explored due to the critical impact that gas composition has on total VOC volumes released, and hence air quality. For example, unprocessed gas typically ranges from 75-90 vol% CH_4, with the rest mainly consisting of VOCs (Baker and Lokhandwala, 2008; Faramawy et al., 2016; Gilman et al., 2013). Wet gas is leaner in CH_4 and richer in VOCs, while the opposite case is true for dry gas. Because it is not known in advance what the gas composition will be, we explore scenarios that cover both wet and dry options. Furthermore, because NO_x emissions are unaffected by gas composition, wet and dry gas scenarios allow us to study the impact of varying levels of VOC loading to NO_x on O_3 production. In our scenarios we applied wet and dry gas compositions of 84.6/15.4 and 96/4 (vol% CH_4/VOCs), respectively, based on Faramawy et al. (2016) and displayed in **Table 3**. Finally, the interest of the latter scenario was to see if NO_x emissions from shale gas activities concentrated in space and time could lead to a significant impact on local O_3 production. Because the conNO_x scenario required further development, it is described in detail in the following section below.

conNO_x scenario design

The purpose of the conNO_x scenario is to explore the sensitivity of the simulation to concentrated NO_x emissions on O_3 production. It needs to be pointed out that absolute NO_x scenario emissions from Cremonese et al. (2019) are not *increased*, but rather *concentrated over space and time*. However, in order to avoid limiting the analysis to an arbitrary segment of the simulation, we run the concentrated NO_x emissions for the entire JJA simulation period. Because the NO_x emissions would be too high over the whole period to look at cumulative metric results, the analysis for the conNO_x scenario is restricted to peak daily values. In this way the model run shows results of concentrated NO_x emissions for any time during the study period, with the advantage being that days with more favorable

Table 3: Wet and dry gas compositions, in vol% (wt% in parentheses)[a]. DOI: https://doi.org/10.1525/elementa.387.t3

Species	Wet gas	Dry gas
CH_4	84.6 (67.1)	96.0 (88.1)
VOCs	15.4 (32.9)	4.0 (11.9)

[a] Data from Faramawy et al. (2016).

Table 2: Shale gas scenarios simulated in this study. DOI: https://doi.org/10.1525/elementa.387.t2

Scenario set	SG1	SG2	SG3
CH_4 leakage[a]	0.70% (UK) 1.36% (DE)	2%	6%
Reference	Cremonese et al. (2019)	Alvarez et al. (2018)	(see text)[b]
Sub-scenarios	dry gas, wet gas, conNO_x	dry gas, wet gas, conNO_x	dry gas, wet gas, conNO_x

[a] The UK and DE have different leakage rates in SG1 due to the design of the drilling projections in (Cremonese et al., 2019). In SG2 and SG3, a flat leakage rate is applied to gas production of both countries.

[b] Based on several different studies in the past years reporting very high CH_4 leakage rates from shale gas activities, as described in the text.

photochemical conditions for O_3 production will automatically be included in the results.

For conNO_x scenario development we first determined which sectors of shale gas exploitation from Cremonese et al. (2019) contribute to NO_x emissions in a manner that a high volume of emissions may be concentrated over space and time. Drilling and fracking activities fit these requirements: both activities require machinery with high horsepower and consequently result in high NO_x emissions, while operation time thereof is relatively short on the order of several days up to a few weeks. Furthermore it is plausible that a contractor would elect to drill/frack multiple wells within the same area, e.g., due to target sweet spots, regulation permits or restrictions, or favorable conditions of a location such as close proximity to roads, pre-existence of pipeline systems etc., so that total NO_x emissions from drilling and fracking activities may be concentrated in space.

According to Cremonese et al. (2019)'s shale gas emission scenarios, drilling and fracking combined constitute approximately 25% of total NO_x emissions for Germany and 20% for the UK. Therefore we concentrate this percentage of NO_x emissions for each respective country, while the rest of the NO_x emissions were treated as in the other scenarios (described in Pre-processing shale gas emissions for WRF-Chem). In our conNO_x scenario we assumed that one well is drilled and one well is fracked per well pad. Based on our calculations, NO_x emissions from drilling and fracking activities are concentrated over an area of 980 km^2 and 1225 km^2, or 8.0% and 7.2% of the total shale gas basin area, for Germany and the UK, respectively. With this information and the time over which the emissions occur, we determined the concentrated NO_x emissions flux. In order to place an upper bound on the effect of concentrated emissions of NO_x, we chose a location for these emissions based on which area exhibited sensitivity to added NO_x emissions for O_3 production. We achieved this through a sensitivity study in which we looked for coordinates within the shale gas basin region which displayed an increase in MDA8 when a simulation included both shale gas VOC and NO_x emissions over a simulation which included shale gas VOCs only (conNO_x regions displayed in **Figure 2**). Nevertheless it is worth noting that the increase displayed by added NO_x emissions was low (<4 $\mu g\ m^{-3}$). Additionally, it is important to note that the conNO_x scenarios are based on wet gas composition like the wet gas scenario (**Table 3**). Further information on the development of and calculations for the conNO_x scenario is provided in SM Text S1, Text S1.

Scenario emissions in context

In order to put our scenario emissions into context, we compare them with TNO MACC III inventory values for year 2011 (**Figure 3**). This offers a useful comparison since the TNO MACC III values are likewise used as anthropo-

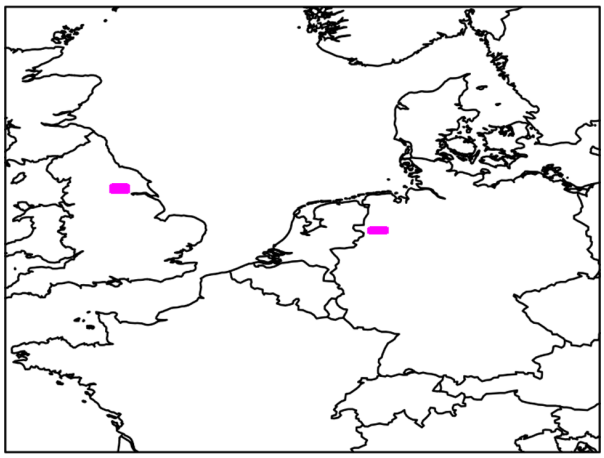

Figure 2: Concentrated NO_x (conNO_x) locations. Masks (in magenta) indicate the locations where NO_x emissions are concentrated in the UK and Germany under the conNO_x scenario. DOI: https://doi.org/10.1525/elementa.387.f2

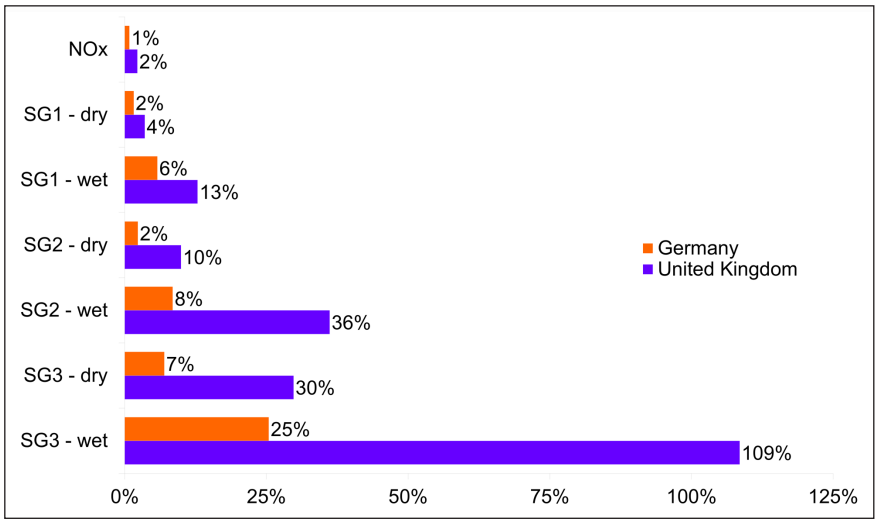

Figure 3: Shale gas scenario emissions compared with country total annual emissions. Scenario emissions are compared as a % equivalent to annual national total emissions from the TNO MACC III inventory, for year 2011. NO_x emissions are presented per country. VOC emissions are presented per scenario set per country, for both 'wet' and 'dry' VOC speciation. DOI: https://doi.org/10.1525/elementa.387.f3

genic emissions input in WRF-Chem (see Model description and emissions). Scenario emissions are equivalent to a higher proportion of country total emissions for the UK than Germany. This is primarily due to British gas production being greater than that of Germany in the scenario storyline. VOC emissions between the scenarios increase greatly from SG1 up to SG3. The importance of gas composition on total VOC emission volumes is evident, where wet gas emissions are about 3–4 times greater than dry gas emissions (more information on wet and dry gas is provided in Present work). With the leakage rate assumed in SG3 under the wet gas scenario, VOC emissions are equivalent to 109% of British country total emissions, and 25% for Germany. In contrast, VOC emissions under SG1 dry gas are equivalent to 4 and 2% of British and German country total emissions.

Pre-processing shale gas emissions for WRF-Chem

The shale gas activities examined in Cremonese et al. (2019) primarily occur within the shale gas basin regions of each respective country. Shale gas emissions from Cremonese et al. (2019) were adapted to the TNO MACC III grid for emissions pre-processing for WRF-Chem (**Figure 4**). The shale gas basin maps for Germany and the UK were obtained from reports by national institutions of each respective country, i.e., the Institute for Geosciences and Natural Resources (*Bundesanstalt für Geowissenschaften und Rohstoffe*) for Germany and the British Geological Survey for the UK (BGR, 2016; BGS, 2013). Because there is currently no commercial shale gas production in these countries, it is not known at which locations shale gas activities will occur and consequently where corresponding emissions will be released; therefore we averaged total scenario emissions over the shale gas basin area for each respective country. The impact of averaging emissions is not expected to be significant since VOCs are relatively long-lived (Atkinson, 2000). Furthermore no considerable diurnal variability in shale gas activities is expected, and accordingly total emissions for each respective country are assumed to occur at a constant rate. The only exception to this is that we concentrated some NO_x emissions over a subset of the shale gas basin region and JJA period, as described in conNO_x scenario design. Averaging the scenario emissions over space and time provided the emission flux for each shale gas species used in our simulations (VOCs, NO_x, and CO from Cremonese et al. (2019). While CH_4 is an important component of shale gas emissions and valuable to the scenario storylines explored here, shale gas CH_4 is not included in our simulations: WRF-Chem treats CH_4 as a BC on account of CH_4's relatively long atmospheric lifetime of circa 12 years (Myhre et al., 2013).

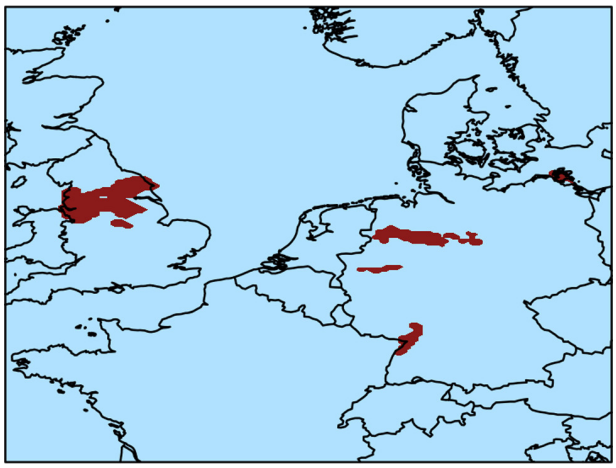

Figure 4: Shale gas basin areas. The basins (maroon) for the UK and Germany represent the areas over which scenario emissions were averaged by country. Corresponding emission fluxes were added to the basin masks and run in scenario simulations with WRF-Chem. Basin areas are based on reports by national institutions, i.e., BGS (UK) and BGR (Germany) (BGR, 2016; BGS, 2013). DOI: https://doi.org/10.1525/elementa.387.f4

In the scenarios explored here, >99.9% of the VOC emissions result directly from natural gas loss. For this reason we applied a typical natural gas VOC composition as the speciation for all VOC emissions from the shale gas scenarios that we pre-processed into WRF-Chem. The VOC speciation for natural gas was obtained from Faramawy et al. (2016) (**Table 4**). Since the MOZART-4 chemical mechanism used in our setup lumps C > 3 alkanes into one group (BIGALK), the actual speciation we applied includes 29% ethane, 35% propane and 36% BIGALK, by weight. We applied the wet gas VOC speciation to all scenarios to avoid confounding the results between wet and dry gas scenarios, i.e., so that wet and dry gas scenarios differ only in their extent of VOC emissions and not in their speciation. It also needs to be pointed out that natural gas is indeed a lightweight mixture of alkanes; nevertheless, in reality gas is often found in the reservoir in association with some oil which contains higher alkanes, alkenes, aromatics, etc. Ahmadov et al. (2015) found that aromatic VOCs have a disproportionately greater contribution to O_3 formation relative to all other VOC emissions. Additionally Carter and Seinfeld (2012) reported that both aromatics and alkenes were the most significant contributors to O_3 formation in spite of their comparatively small

Table 4: Natural gas VOC speciation applied to emissions during pre-processing for WRF-Chem, in % wt[a]. DOI: https://doi.org/10.1525/elementa.387.t4

Species	Faramawy et al. (2016)	MOZART-4
Ethane	29%	29%
Propane	35%	35%
Isobutane	10%	36% (BIGALK)
n-butane	12%	–
Isopentane	4%	–
Pentane	2%	–
Hexanes	5%	–
Heptanes	2%	–

[a] Values displayed adapted from the Faramawy et al. (2016) composition for wet gas for use with MOZART-4.

VOC contribution. Therefore if oil is present, the impact of VOCs on O_3 production may be even greater.

Results and discussion

Evaluation

Due to the similarity of our setups, we use the same approach and offer a comparison of our evaluation results to those of Mar et al. (2016). Notable differences between our setup and Mar et al. (2016) include the following (our setup/Mar et al., 2016): WRF-Chem versions (3.8.1/3.5.1), simulation years (2011/2007), anthropogenic emissions inventory (TNO MACC version III/TNO MACC version II), horizontal resolutions (15 km × 15 km/45 × 45 km), and European domain coverage (Western Europe/whole of Europe). It is worth emphasizing that the principle goal of this study is to quantify the impacts of shale gas production on air quality by means of a reasonably working setup; because an in-depth evaluation is provided by Mar et al. (2016), we focus on main findings here.

The meteorological observations used for evaluation are taken from the Global Weather Observation dataset provided by the British Atmospheric Data Center (BADC) (Met Office, 2006). The chemical observations are taken from AirBase, the European air quality database of the European Environmental Agency (EEA, 2013). Like Mar et al. (2016) we compare our data to rural background stations since our horizontal grid resolution is likewise relatively course and therefore more representative of rural conditions. We evaluate our model-simulated results against observations for the following statistics: mean model, mean observations, mean bias (MB), normalized mean bias (NMB), mean fractional bias (MFB), and the temporal correlation coefficient (*r*). Definitions of the statistical calculations are provided in Mar et al. (2016).

Meteorology

The meteorological evaluation was carried out for the following variables at a 3-hourly temporal resolution: mean sea-level pressure (MSLP), 2m temperature (T2), and 10m wind speed and direction (WS10 and WD10, respectively). A summary of the domain-wide statistical performance for meteorology of the base run setup with WRF-Chem against the observations at rural background stations is shown below in **Table 5**.

MSLP was reproduced over the domain with a high degree of accuracy. The bias for MSLP is negligible, where both NMB and MFB are 0, and the *r* value is 0.99. Likewise T2 was found to be reproduced with a high degree of accuracy by WRF-Chem, with a low MB of –0.08°C averaged over the entire domain. The seasonal average T2 spatial distribution statistics are displayed in **Figure 5**. In general the absolute values of MB in T2 (**Figure 5C**) were <1°C, where larger biases are found in the Alps. This greater bias over mountainous regions was also found in Zhang et al. (2013a) and Mar et al. (2016), which the latter notes is likely due to the complex mountain terrain and related unresolved local dynamics. Moreover the *r* values for T2 (**Figure 5D**) are generally >0.9 and do not display considerable geographical variation, which demonstrates the models ability to reproduce this parameter well. Furthermore it was found that the model represents wind speed well, with a domain-wide average MB of +0.07 $m \cdot s^{-1}$ and *r* value of 0.67. Averaged wind direction over the domain was found to originate from the south-west, with a MB of about 20 degrees (a wind rose diagram for model results over JJA has been provided in SM Text S1, Figure S1). In total, it was found that our WRF-Chem set-up is capable of reproducing meteorological conditions and their spatial and temporal variations in Europe reasonably well, and notably our values are consistent with those reported in, e.g., Zhang et al. (2013a) and Mar et al. (2016).

Chemistry

We performed an evaluation of the model chemistry with hourly observations of the following species: O_3, NO_x, NO_2 and NO. The domain-wide statistical performance for chemistry of the base run setup with WRF-Chem against the observations at rural background stations is shown below in **Table 6**.

In **Figure 6** we see that the lowest modeled surface O_3 concentrations in our domain are concentrated over the UK, Belgium, the Netherlands and the North Rhine-Westphalia region of Germany, with averaged values around 50–60 μg m^{-3}, while highest over the Mediterranean region, where values exceed 110 μg m^{-3}. O_3 is overpredicted throughout most of Italy; similarly, high O_3 was predicted over the Mediterranean with WRF-Chem in Mar et al. (2016) and with various models in Im et al. (2015). This finding may be due to the relatively coarse model resolution causing an underestimation of NO_x and in turn an overestimation of O_3, or causing an excessive diffusion of O_3 from the sea to the land. Predicted O_3 concentrations reproduce the north-south gradient shown in the observations. In **Table 6**, we see that our WRF-Chem setup overpredicts O_3 with a MB

Table 5: Domain-wide statistics of WRF-Chem base run setup against BADC 3-hourly meteorological observations, over JJA. DOI: https://doi.org/10.1525/elementa.387.t5

Meteorological variables	Mean-Obs[a]	Mean-Mod[a]	MB[a]	NMB[b]	MFB[b]	*r*[b]	No. stations
MSLP (hPa)	1013.43	1013.52	0.09	0.00	0.00	0.99	1332
T2 (°C)	16.93	16.85	–0.08	0.00	0.01	0.91	1629
WS10 ($m \cdot s^{-1}$)	3.45	3.52	0.07	0.02	0.14	0.67	1631
WD10 (°)	210.00	229.89	19.89	0.11	0.21	0.5	1619

[a] Means and MB are in units indicated next to meteorological variable.
[b] NMB, MFB and *r* are unitless.

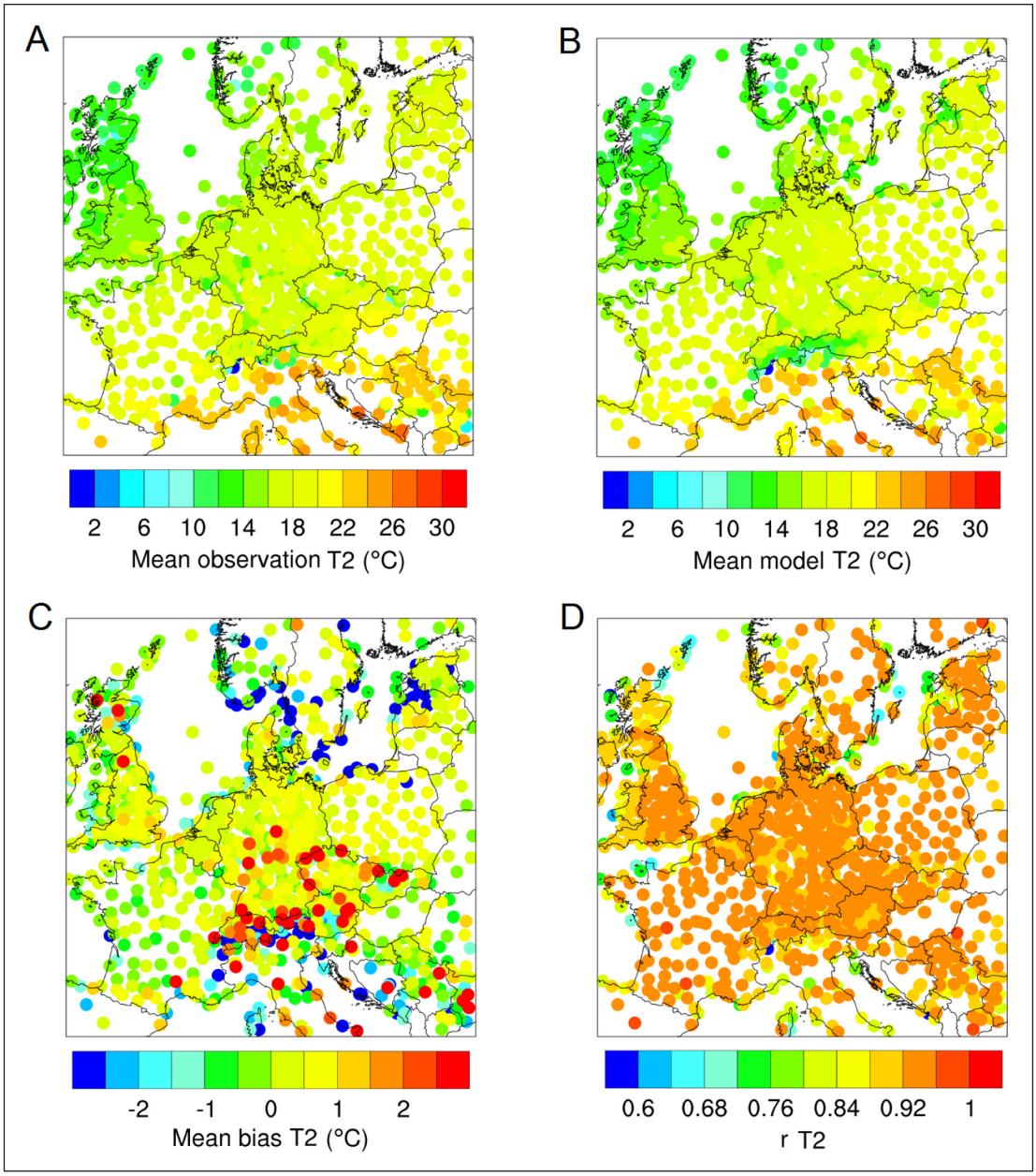

Figure 5: Seasonal average (JJA) 2m temperature (T2) spatial distribution statistics. Model values and statistics: **(A)** mean observation, **(B)** mean model, **(C)** mean bias, and **(D)** temporal correlation coefficient, are shown at the location of the observations. Results for means and MB are in °C, while *r* is unitless. DOI: https://doi.org/10.1525/elementa.387.f5

Table 6: Domain-wide statistics of WRF-Chem base run setup against AirBase hourly chemical observations, over JJA. DOI: https://doi.org/10.1525/elementa.387.t6

Species	Mean-Obs[a]	Mean-Mod[a]	MB[a]	NMB[b]	MFB[b]	$r^{b,c}$	No. stations
O_3	70.21	80.11	9.90	0.14	0.19	0.52	429
MDA8	91.64	96.97	5.33	0.06	0.07	0.63	429
NO_x	8.65	8.38	–0.27	–0.03	–0.20	0.22	283
NO_2	6.59	7.6	1.01	0.15	–0.12	0.27	298
NO	1.47	0.54	–0.93	–0.63	–1.07	0.23	216

[a] Means and MB are in units of μg m^{-3}.
[b] NMB, MFB and *r* are unitless.
[c] *r* represents the hourly temporal correlation coefficient for species O_3, NO_x, NO_2, and NO, while for MDA8 it represents the daily temporal correlation coefficient.

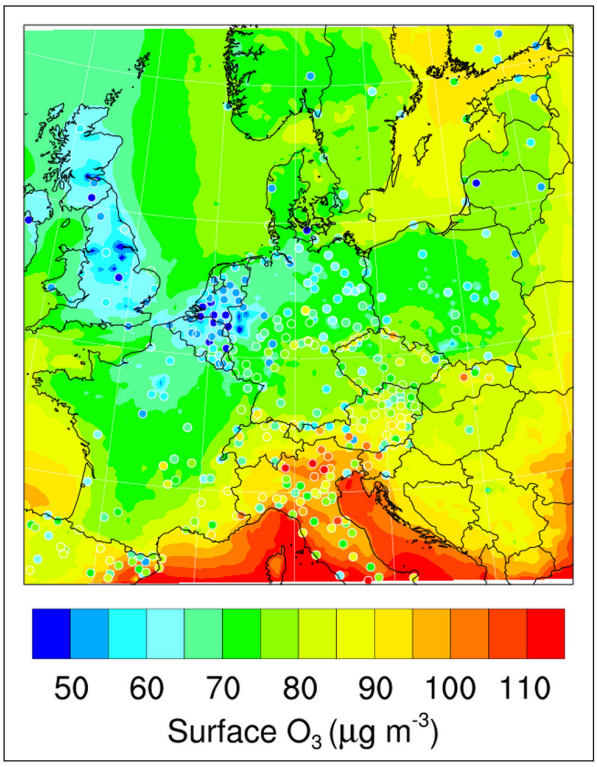

Figure 6: Seasonal surface-averaged O_3. Contours are modeled values and dots represent observational values measured at station locations, over JJA, in units of µg m^{-3}. DOI: https://doi.org/10.1525/elementa.387.f6

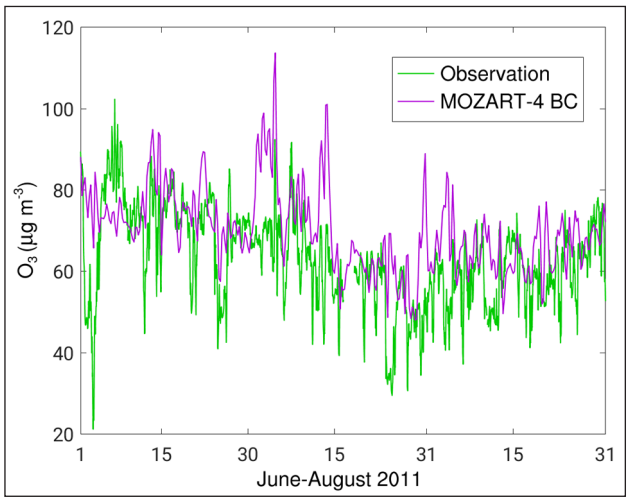

Figure 7: Time series of O_3 for boundary condition assessment at Mace Head Station. Hourly BADC observational data (green) are compared with 6-hourly MOZART-4 boundary condition modeled data (purple), over JJA, in units of µg m^{-3}. DOI: https://doi.org/10.1525/elementa.387.f7

of 9.90 µg m^{-3} and NMB of 0.14, similar to those reported in Mar et al. (2016) for the JJA season (MB: 9.92 µg m^{-3}; NMB: 0.14). Moreover, our results are consistent with other regional modeling studies for Europe, e.g., the absolute NMB values for O_3 in ensemble modeling studies of the Air Quality Model Evaluation International Initiative (AQMEII), e.g., Solazzo et al. (2012b) for the summertime and Im et al. (2015) for year 2010. Additionally the NMB value is within the model performance criteria by Russell and Dennis (2000) for O_3, for which normalized mean bias is suggested to be within a range of ±5 to 15%. Our temporal correlation value for O_3 is 0.52, which is consistent with Mar et al. (2016)'s value of 0.55 and Tuccella et al. (2012), who reported an hourly correlation value of 0.62 averaged over the year 2007. Also in **Table 6** we see that our setup slightly overpredicts MDA8, though our MB for MDA8 is lower than that for O_3. Since MDA8 is essentially a measure of daytime O_3, this indicates that our setup is performing very well predicting O_3 values during the day, but overpredicts O_3 nighttime values to a greater extent, possibly due to NO_x titration during the nighttime not being as well resolved by the model.

Due to the model overestimation of O_3, we provide a brief assessment of the O_3 BC (boundary condition) used in this study provided by the MOZART-4 global model (described in Model description and emissions) at Mace Head station. Mace Head is located on the west coast of Ireland making it less likely to be influenced by European emissions, and therefore representative of the background O_3 flowing into Europe. In **Figure 7** is depicted a time series plot comparing hourly observational (BADC) data with 6-hour O_3 BC data, over JJA. The O_3 BC slightly overpredicts background O_3, and occasionally overestimates O_3 peaks. The O_3 BC does not capture the drops in the observed O_3 which can be caused by the coarse resolution of the model (1.9 × 2.5 degrees). This finding is consistent with previous work of Pfister et al. (2011): in their study looking at summertime pollution inflow into California, they found that the O_3 BC from the MOZART-4 global model overpredicts measured background O_3. On the other hand, the large drops in observed O_3 not seen in the O_3 BC could be due in part to the influence of local NO_x sources, since the observational data at Mace Head station have not been filtered for background air. The O_3 BC likely contributes to the positive bias in O_3 found in statistical evaluation results for O_3 and MDA8 (**Table 6**) through transport of background O_3 via the westerly winds (HTAP, 2010). Overall, however, the O_3 BC compares well with the observational time series trend.

In **Figure 8** high NO_x concentrations (~30 µg m^{-3} and greater) are visible over parts of the UK, the Netherlands, Belgium, Germany, Poland, and large urban conglomerates like Paris, Barcelona, and Belgrade, as well as the coastal region where the English channel meets the North Sea, resulting from high emission activities in these areas. In **Table 6** we see that our setup slightly underestimates domain-average NO_x concentrations (MB: –0.27 µg m^{-3}) over JJA due to the balancing of underestimated NO (MB: –0.93 µg m^{-3}) and overestimated NO_2 (MB: 1.01 µg m^{-3}). Our results for JJA are consistent with NO_2 (over-) and NO/NO_x (underprediction) trends for the whole year reported in Mar et al. (2016). These biases are likely a combination of uncertainty in NO_x emissions (Kuenen et al., 2014) and in the model representation. Reported causes of the latter include deficiencies in mixing in the planetary boundary layer (Kuik et al., 2018), overestimating

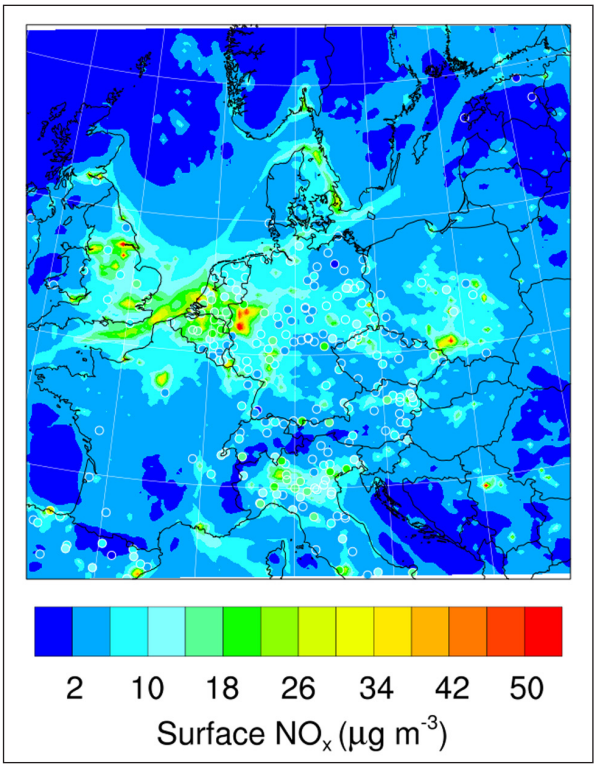

Figure 8: Seasonal surface-averaged NO_x. Contours are modeled values and dots represent observational values measured at station locations, over JJA, in units of µg m^{-3}. DOI: https://doi.org/10.1525/elementa.387.f8

nighttime NO_2 (Im et al., 2015), coarse grid resolution (Kuik et al., 2018), and that the atmospheric lifetime may be too long relative to deposition or chemical loss mechanisms (Stern et al., 2008). In the AQMEII project Im et al. (2015) found NO_2 to be overestimated by one model by 15%, while underestimated by the rest of the models by 9 to 45% for the European domain, where the WRF-Chem simulations used RADM2, CBMZ (Zaveri and Peters, 1999), RACM (Stockwell et al., 1997) mechanisms. In their model inter-comparison study on Central Europe, Stern et al. (2008) found both over- and underpredictions for NO_2 from 15 January 2003 to 5 April 2003. (Note that the aforementioned studies do not perform a validation for NO or NO_x). The domain average JJA temporal correlation coefficients against hourly NO_x, NO_2 and NO measurements are 0.22, 0.27 and 0.23, respectively. These *r* values are lower than that of O_3, but consistent with Mar et al. (2016) who reported values of 0.16, 0.22 and 0.19, respectively. Low *r* values as seen here indicate that the model is not suitable for predicting exceedances of NO_2. The generally low *r* values for NO_x are likely the result of model resolution, strong temporal variation of NO_x emission sources, and unreliable model inputs such as emissions (Karlický et al., 2017).

Overall, we find that the model performance for chemistry is consistent with Mar et al. (2016) on which we based our setup, and furthermore in line with biases of other studies for Europe, e.g., Solazzo et al. (2012b), Tuccella et al. (2012) and Im et al. (2015). Based on these aspects we find that our setup is performing at a reasonable level for modeling the impact of shale gas industry emissions on European air quality.

Quantification of O_3 impacts from shale gas activities

The maximum difference in daily MDA8 between scenario and base case, over the entire simulation period for each grid cell (referred to as ΔMDA8), is depicted in **Figure 9**; statistical data is provided in SM Text S1, Table S2. Note that in the following discussion we generally leave out SG2 to be concise as its impacts fall between the SG1 and SG3 cases.

In the SG1 wet gas scenario, predicted ΔMDA8 generally ranges between 2–4 µg m^{-3} and is restricted to relatively small areas located within the vicinity of the shale gas basin regions. Concentrating NO_x emissions leads to prominent differences compared with averaging NO_x emissions under SG1: ΔMDA8 values >2 µg m^{-3} stretch over a larger area for $conNO_x$, especially over Germany and within the vicinity where NO_x emissions are concentrated. The peak values likewise show a stark difference, where peak ΔMDA8 for wet gas is 4.5 µg m^{-3} and for $conNO_x$ is 9.5 µg m^{-3}. This indicates model O_3 sensitivity to NO_x, especially in Germany. In the dry gas scenario, ΔMDA8 values are lower compared with wet gas and are more strictly located over the shale gas regions, showing the importance of VOCs in model O_3 formation.

Under SG3 with wet gas speciation the largest peak ΔMDA8 occurs, reaching 28.3 µg m^{-3} and located over the North Sea off the British coast. This result is consistent with Archibald et al. 2018, where the largest maximum increase in MDA8 occurs under the scenario with the greatest VOC emissions. Also notable is that peak ΔMDA8 under SG3 is seen in the wet gas scenario; this is in contrast to SG1, where peak ΔMDA8 occurs in the $conNO_x$ scenario. Nevertheless, $conNO_x$ and wet gas are relatively similar under SG3, which also stands in contrast to SG1. ΔMDA8 values >2 µg m^{-3} extend over a considerably greater area of the domain for the wet gas and $conNO_x$ scenarios under SG3 compared with their SG1 counterparts, reaching Scandinavia, Eastern Europe, and the Mediterranean countries. ΔMDA8 values are especially prominent in marine areas including the Baltic Sea, the Mediterranean Sea, and the Atlantic Ocean west of the UK (in addition to the North Sea). Further under SG3 wet gas and $conNO_x$ scenarios, most of the UK experiences ΔMDA8 values >6 µg m^{-3} near the coast, with the inner portion of the country seeing enhancements from 14 up to about 22 µg m^{-3}. In Germany, the majority of the country experiences ΔMDA8 values >2 µg m^{-3}, with Northern Germany experiencing the highest values from 8 to 12 µg m^{-3} (SG3), in part due to the majority of the shale gas basin area being located in the upper half of the country. The much greater impact on MDA8 in the UK compared with Germany is likely due to VOC shale gas emissions being much higher in the UK (**Figure 3**); this is a result of the British shale gas industry being about three times larger than Germany in terms of gas production according to the scenarios. Additionally, under SG3 many of the neighboring countries experience high O_3 enhancement maxima likely due to long-range

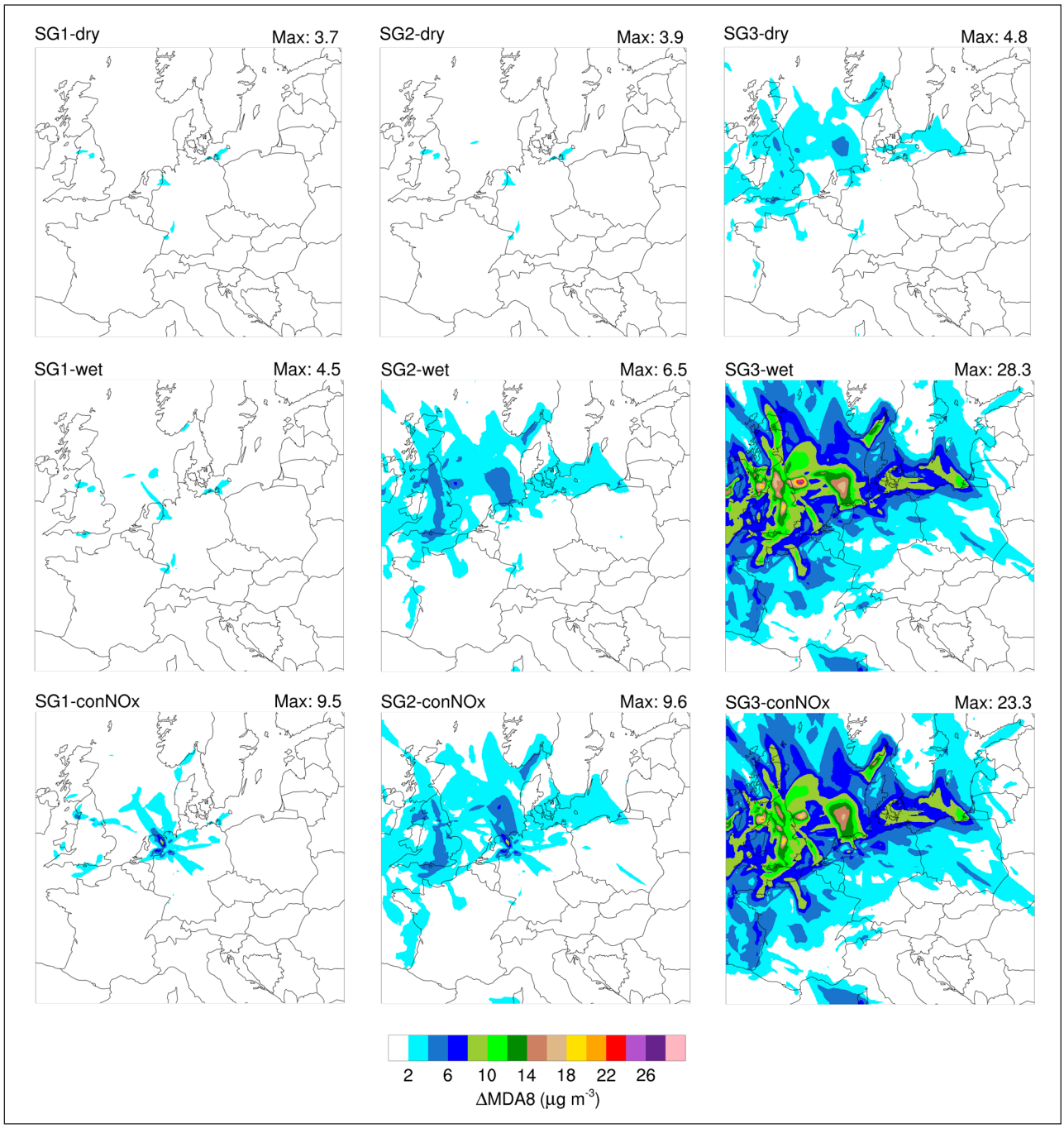

Figure 9: Maximum seasonal enhancement of scenarios on MDA8 (maximum daily 8-hour average O_3). Plots represent ΔMDA8, defined here as the maximum difference in MDA8 between the shale gas scenarios and base case over JJA, for each cell, in units of μg m^{-3}. The top left-hand corner of each plot indicates the particular scenario, and the top right-hand corner displays the peak ΔMDA8 value experienced over the domain and simulation period.
DOI: https://doi.org/10.1525/elementa.387.f9

transport: Belgium, Denmark, and Norway have ΔMDA8 values up to 8–10 μg m^{-3}, France and Northern Ireland 8–12 μg m^{-3}, Kalingrad Oblast region of Russia 12–14 μg m^{-3}, and Ireland and the Netherlands 12–16 μg m^{-3}. Notably, the portion of Italy in our domain experiences ΔMDA8 values of only ~2–4 μg m^{-3}. It is interesting to note here that the weather over Europe during the simulation period was dominated by cyclonic fields (low pressure systems). Low pressure systems are generally associated with clouds, storms, and wind. In this case it means that the shale gas O_3 impacts would be more widespread, as seen in the results here. Finally, ΔMDA8 values for dry gas under SG3 are markedly less in extent and magnitude compared with wet speciation (i.e., wet gas and conNO$_x$ scenarios).

These results show that the O_3 enhancement resulting from shale gas activities taking place inside the UK and Germany can be significant, with the potential to negatively affect air quality on the local and regional scales in Europe. The general trend of model O_3 here is that as shale gas VOC emissions increase from SG1 up to SG3 and from dry gas to wet gas speciation (wet gas and conNO$_x$),

O_3 maxima increase considerably in magnitude as well as in extent over the domain. Total VOC emissions from shale gas activities (as a result of gas composition and leakage) are critical in increasing local and regional O_3 over the base case. Interestingly, when VOC emissions are relatively low (SG1), concentrating NO_x emissions leads to greater O_3 increase in magnitude and extent than when NO_x emissions are averaged; however, when VOC emissions are relatively high (SG3) O_3 maxima outcomes are similar when NO_x emissions are concentrated or averaged. This variance in model O_3 sensitivity to NO_x under different VOC loadings is likely the result of the nonlinear relationship between O_3 precursors and its formation in the atmosphere. Further the fact that concentrating NO_x emissions leads to similar or slightly greater O_3 than averaged NO_x emissions indicates a mixed regime of sensitivity to both NO_x and VOC; though, varying NO_x leads to a lower impact overall on O_3 than varying VOC emissions does. In sum, the most critical factor on increasing local and regional O_3 over the base case is the amount of VOC emissions, while concentration of NO_x emissions plays a further, albeit minor, role.

Next we explore extra exceedances of MDA8 at the locations of regulatory measurement stations, namely those which otherwise would not occur but do so as a result of shale gas activities. Here we explore the EU threshold due to its relevance for regional regulations of the study area, and examine the WHO guidelines due to the more comprehensive scope of health as well as international relevance. On account of inherent model bias in MDA8, which in our case is low yet nevertheless present, we calculate extra exceedances by the following: where an observational value is below the threshold, the difference in MDA8 between the base case and scenario at the measurement location is added to the observational value, and, when these two values together surpass the threshold, this is treated as an extra exceedance. Henceforth, we refer to these as exceedances for ease of discussion. AirBase measurement stations considered within our domain have at least 75% temporal data coverage for the JJA simulation period ("valid stations"). In the interest of clarity, it is worth noting that for countries not fully covered by the domain (e.g., Italy), only the stations of that country that are located within the domain are included in our analysis.

Figure 10 depicts the total exceedance counts, summed over the full set of valid stations, under the WHO and EU thresholds. The number of exceedances increases

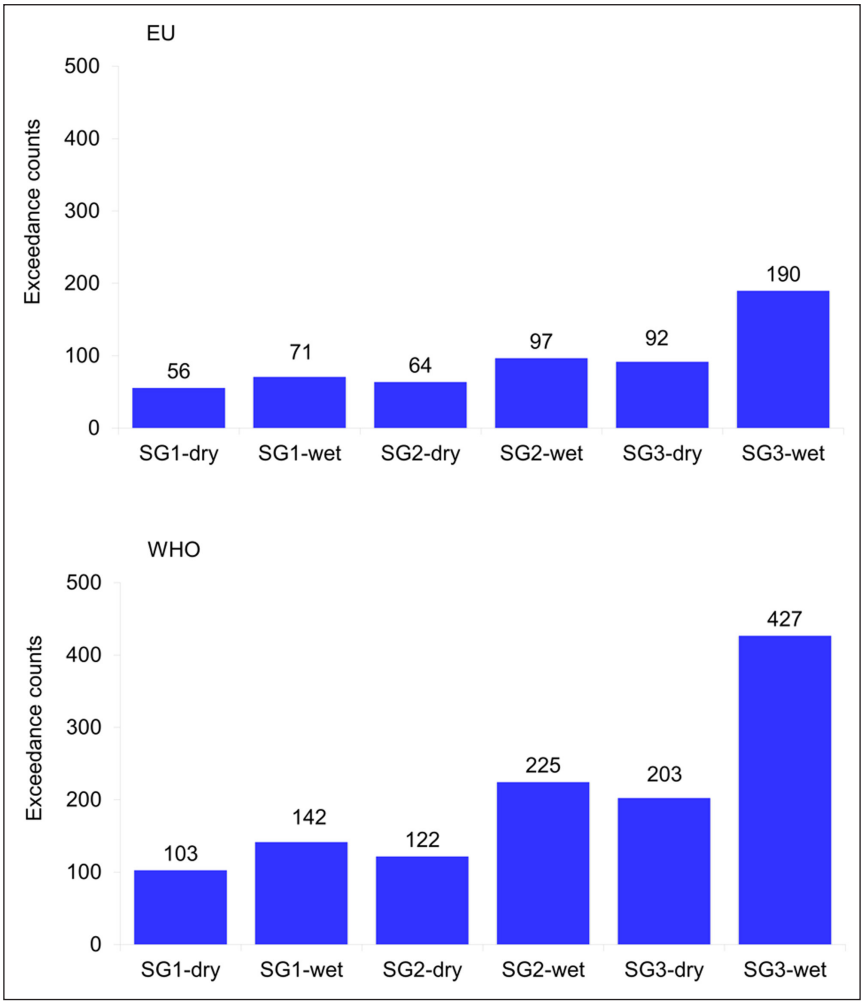

Figure 10: Total O_3 exceedance counts per scenario. The number of extra exceedances predicted as a result of O_3 enhancement from shale gas scenario emissions, over JJA, applying the EU and WHO thresholds for O_3 (120 and 100 μg m^{-3} respectively), summed over all AirBase stations within our domain that have at least 75% temporal data coverage. DOI: https://doi.org/10.1525/elementa.387.f10

substantially over the lower WHO threshold value compared with the EU threshold value, ranging from 56 to 190 (EU threshold) and from 103 to 427 (WHO threshold); this highlights the impact of the threshold value on the total number of exceedances registered. Further we see that exceedances increase considerably as VOC emissions increase: under both thresholds, the lowest number of exceedances occurs in the lowest VOC scenario (SG1-dry gas) while the greatest number of exceedances in the highest VOC scenario (SG3-wet gas). In order to put these exceedance counts into context, we examine the number of exceedances per station and then in **Table 7** present data on the percentage of stations in each country which have exceedances. The exceedances caused by the scenario emissions are spread out among the stations, rather than a few stations experiencing the majority of exceedances. The mean number of exceedances per station under all scenarios is 1 (not including stations which exhibit zero exceedances), where the maximum exceedance experienced at any station is 2–3. This demonstrates the widespread, episodic nature of shale gas emissions on station exceedances. Additionally it shows that while shale gas activities, even under extreme emission cases, have the potential to cause considerably more exceedances over large areas, the frequency of this effect on any particular station or area is low in this regard. Due to the similarity in trends when applying the EU and WHO thresholds, we show exceedances from here on applying the WHO threshold for the sake of brevity; data for the EU threshold is provided in SM Text S1, Table S3.

The number of stations with valid data over our simulation period varies strongly from country to country within our domain (**Table 7**). France has the highest number of valid stations (386) followed by Italy (244), of which 8–33% and 9–18% show exceedances, respectively (representing SG1-dry gas at the low end of the range and SG3-wet gas at the high end). Germany has the third highest number of valid stations (234), of which 6 to 21% of these stations have exceedances (SG1-dry gas to SG3-wet gas). 80 valid stations are located in the UK, of which 4–35% encounter exceedances (SG1-dry gas to SG3-wet gas). The higher percentage of British stations having exceedances

Table 7: Stations per country and exceedance data per country with respect to the WHO threshold, over JJA. DOI: https://doi.org/10.1525/elementa.387.t7

Country		SG1				SG2				SG3			
		dry gas		wet gas		dry gas		wet gas		dry gas		wet gas	
	Σ_c [a]	Σ_e [b]	%[c]	Σ_e	%	Σ_e	%	Σ_e	%	Σ_e	%	Σ_e	%
France	386	29	8	44	11	39	10	76	20	69	18	127	33
Italy	244	23	9	26	11	23	9	32	13	29	12	45	18
Germany	234	13	6	17	7	15	6	29	12	27	12	50	21
Spain	129	5	4	5	4	5	4	7	5	7	5	13	10
Austria	111	4	4	4	4	4	4	6	5	4	4	14	13
U. Kingdom	80	3	4	6	8	3	4	12	15	11	14	28	35
Poland	61	6	10	7	12	6	10	11	18	10	16	18	30
Czech Rep.	60	6	10	9	15	8	13	11	18	10	17	22	37
Belgium	42	0	0	1	2	0	0	2	5	2	5	6	14
Switzerland	30	3	10	5	17	4	13	6	20	5	17	9	30
Hungary	17	2	12	2	12	2	12	3	18	2	12	3	18
Netherlands	15	0	0	1	7	0	0	2	13	1	7	6	40
Macedonia	12	0	0	0	0	0	0	0	0	0	0	1	8
Slovenia	12	2	17	2	17	2	17	2	17	2	17	3	25
Sweden	12	0	0	1	8	1	8	1	8	1	8	1	8
Finland	11	1	9	1	9	1	9	1	9	1	9	1	9
Slovakia	11	0	0	0	0	0	0	0	0	0	0	1	9
Latvia	8	0	0	0	0	0	0	0	0	0	0	1	13
Denmark	7	1	14	1	14	1	14	2	29	2	29	4	57
Luxembourg	6	0	0	0	0	0	0	0	0	0	0	1	17

[a] Number of stations with valid measurements per country. Only country stations which are located within the model domain are included in the analysis.
[b] Number of stations that experience exceedances per country.
[c] Percentage of stations per country that have an exceedance.

compared with German stations is the result of the majority of the UK having a relatively high ΔMDA8 compared with Germany from shale gas emissions (**Figure 9**). Again, as VOC emissions increase from SG1 to SG3 and from dry gas to wet gas, exceedances generally increase. Furthermore stations in distant countries have exceedances as a result of long-range transport, e.g., Macedonia, Slovakia and Latvia. Based on these findings shale gas activities have the potential to cause exceedances at a considerable percentage of country stations (locally and in distant countries), where VOC emissions are critical to the extent of exceedances.

Plots of exceedance magnitude are presented in **Figure 11** applying the WHO guideline, and in SM Text S1, Figure S2 applying the EU threshold. We define exceedance magnitude as the difference between the scenario and base case when an exceedance occurs. This provides meaningful insight because it shows whether shale gas activities only effected an exceedance because the background O_3 concentration was already very close to the limit value (i.e., when exceedance magnitude is low), or whether shale gas activities had a robust impact on MDA8 during an exceedance (i.e., when exceedance magnitude is high). The maximum exceedance magnitude spans between 0.8 to 15.1 μg m^{-3} under the WHO threshold. Exceedance magnitudes are low (mostly <1 μg m^{-3}) in SG1, indicating that low shale gas VOCs are able to force an exceedance only when the background O_3 level is already close to the threshold. These results again reflect that the lower VOC scenarios lead to a low impact, whereas the impact is stronger with the high VOC scenarios.

While Italy is one of the top exceedance locations among the scenarios, it exhibits a very low exceedance magnitude, where in all scenarios the majority of values are <1 μg m^{-3}, with only a few values exceeding this value yet are still below 2 μg m^{-3}. This implies that background MDA8 levels are already high in Italy and close to the limit value, so that only a slight increase in MDA8 from shale gas through long-range transport is required to push it over. Consequently this results in many exceedances occurring in Italy (**Table 7**) in spite of being further away from the shale gas activity area and experiencing a low overall

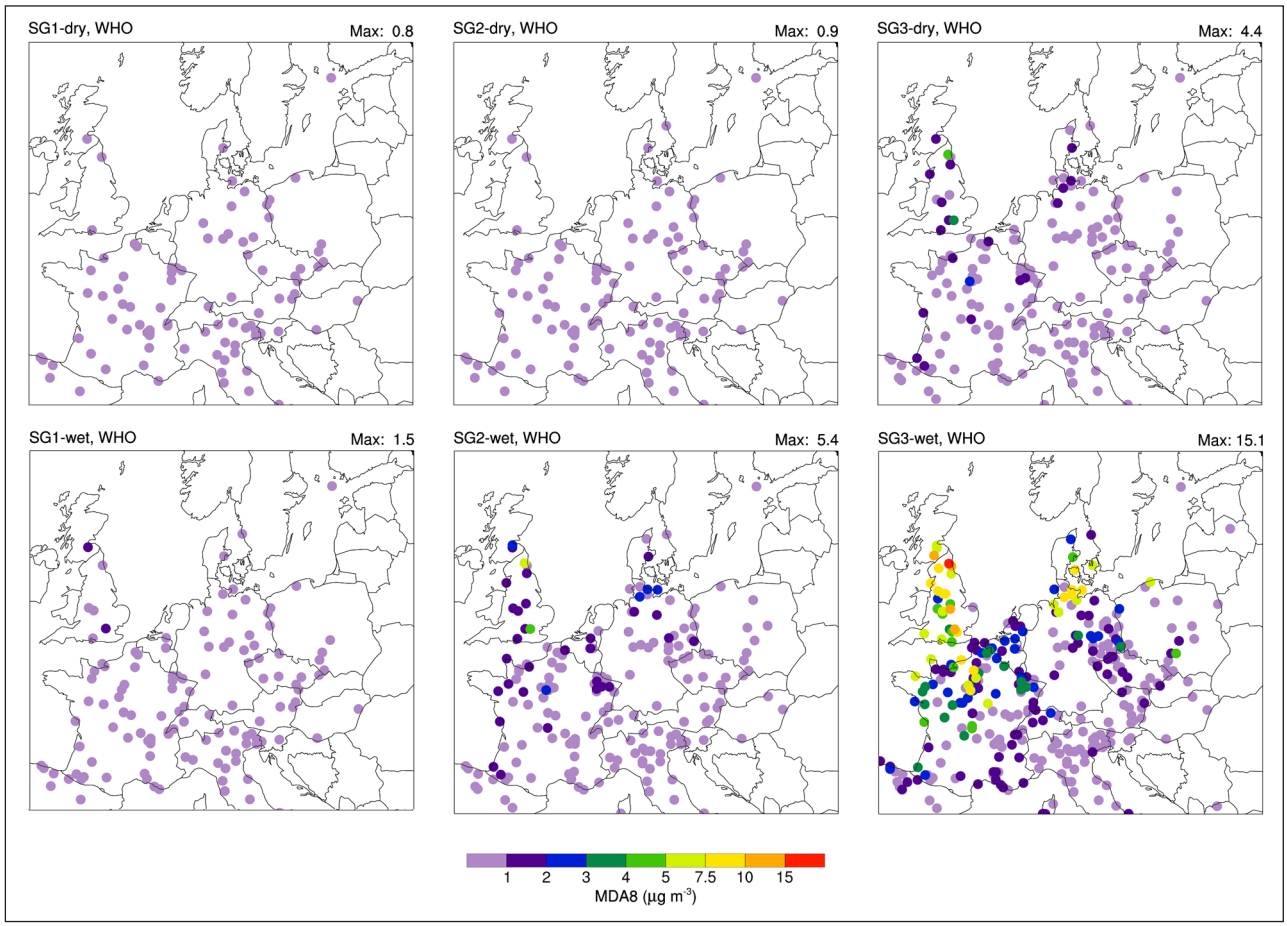

Figure 11: Spatial depiction of exceedances and corresponding exceedance magnitude. Exceedance magnitude is defined as the difference between the shale gas scenarios and base case when an exceedance occurs, and is an indicator of the robustness of shale gas emissions on an exceedance. Exceedances are displayed as filled dots at the station locations where they occur, in μg m^{-3}, over JJA, applying the WHO guideline for O_3 as the threshold (100 μg m^{-3}). For stations which experienced more than one exceedance, the maximum exceedance magnitude is shown. The top left-hand corner of each plot indicates the particular scenario, and the top right-hand corner displays the maximum exceedance magnitude value experienced over the domain and simulation period. DOI: https://doi.org/10.1525/elementa.387.f11

ΔMDA8 (**Figure 9**). The UK displays the highest exceedance magnitude of the countries in our domain, where maximum values reach >15 μg m^{-3} under SG3. This finding is in line with the surface plots displayed in **Figure 9**, which show that ΔMDA8 is highest in the UK among all countries in the domain; again, this is likely due in part to the shale gas industry and consequently VOC scenario emissions being highest in this country. The exceedance magnitude for France is relatively high under the greater VOC scenarios, which is not surprising because of its close proximity to the shale gas activity areas of both the UK and Germany and high ΔMDA8 (**Figure 9**). Additionally, France experiences a greater number of high magnitude exceedances than does Germany. This is not surprising considering that relatively high ΔMDA8 (4–6 ppb) covered a greater area in France than Germany (**Figure 9**).

SOMO35 is an indicator of accumulated O_3 exposure recommended by the WHO for use in health impact assessment, and is the sum of O_3 values exceeding an MDA8 level of 35 ppb or 70 μg m^{-3} (Equation 1) (Amann et al., 2008). The 35 ppb cutoff was chosen because the relationship between O_3 and negative health effects, as well as atmospheric models, is very uncertain below this threshold (WHO, 2013).

Equation 1

$$\mathrm{SOMO35} = \sum_{i\mathrm{day}} \max\left(0, C_{i\mathrm{day}} - 70\,\mu\mathrm{g\,m^{-3}}\right)$$

where $C_{i\mathrm{day}}$ is the maximum daily 8-hour average concentration and the summation is from i_{day} = 1 to 92 for the JJA simulation period.

Surface plots showing the percent impact of each scenario on SOMO35 levels are presented in **Figure 12**. A surface plot showing SOMO35 values for the base case is provided in SM Text S1, Figure S3. In the base run, a north-south gradient of increasing SOMO35 is apparent, where values reach as high as 7500 μg/m^3 days in some parts over the Mediterranean Sea. Under the SG1 scenario set, a low increase in SOMO35 is present over the entire domain (generally less than 1%), while slightly greater increases are localized to the German shale gas basin regions and some of the area north of the British basin. Largely in contrast with the German basins, over the British basin area

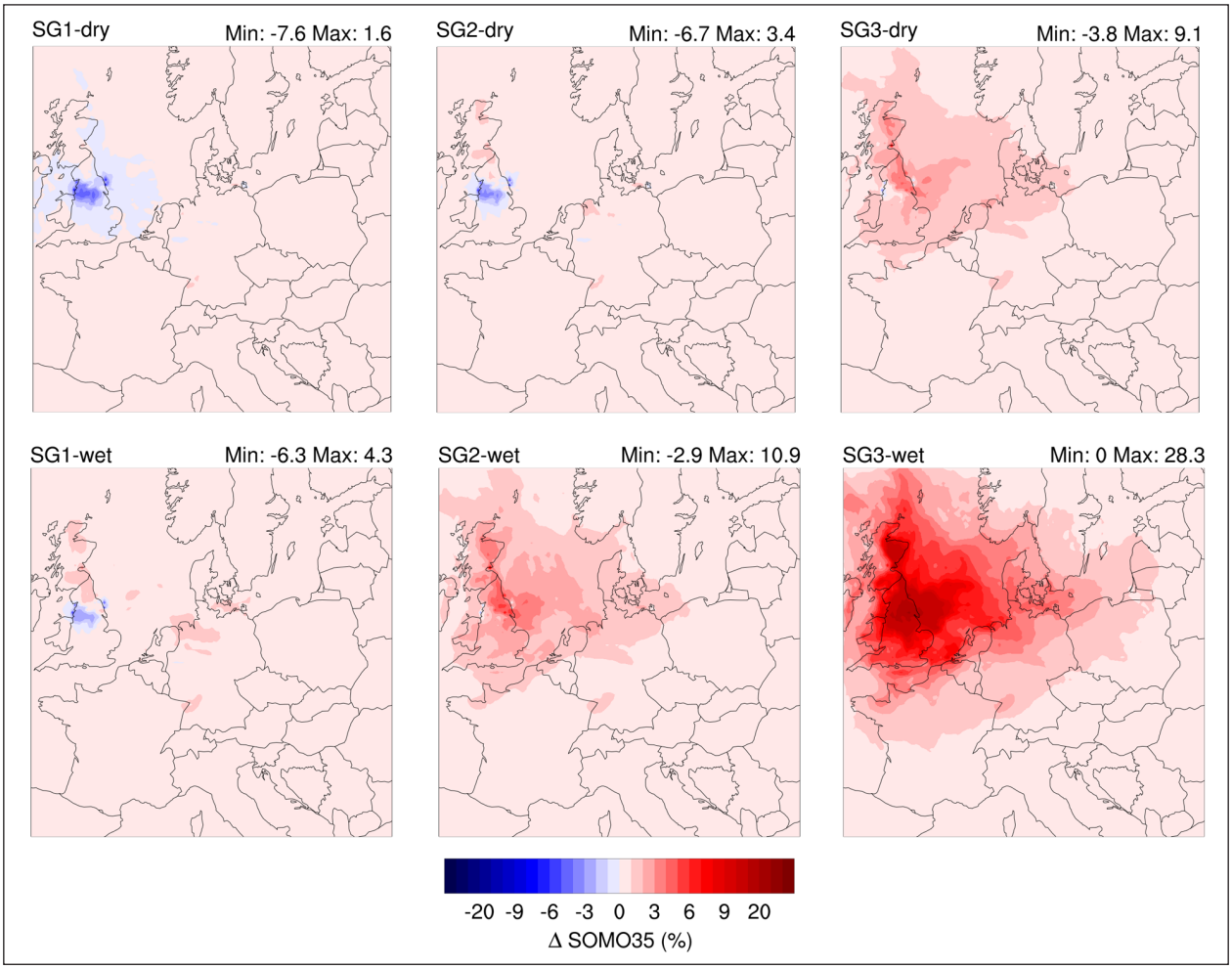

Figure 12: Percent change in SOMO35 (annual Sum of Ozone Means Over 35 ppb, daily maximum 8-hour) from scenarios compared with the base case, over JJA. SOMO35 is an indicator of accumulated O_3 exposure. The top left-hand corner of each plot indicates the particular scenario, and the top right-hand corner displays the minimum and maximum percent changes in SOMO35 values experienced over the domain. DOI: https://doi.org/10.1525/elementa.387.f12

there is a prominent decrease in SOMO35 as a result of NO_x titration. However, because the UK already experiences relatively low values of SOMO35 (SM Text S1, Figure S3), this is not expected to bring about substantial health benefits there through reduced O_3 exposure. The maximum percent increase in SOMO35 for dry gas under SG1 is only slightly less compared with wet gas, though the percent decrease covers a considerably greater area on account of greater NO_x titration due to less VOCs.

Under SG2 (wet gas) and SG3, greater increases in SOMO35 stretch over a more extensive area of the domain over the UK and Northern Germany and the surrounding region (with effects most concentrated over the UK and the North Sea). Notably, the southern portion of the domain experiences a very low percent increase meaning that VOC emissions are not expected to cause relatively worse health impacts on this region. Under SG3 wet gas, there is essentially no percent decrease in SOMO35 on account of less NO_x titration due to greater VOC emissions. The impact of VOC emissions on SOMO35 values is clear, which reach a maximum percent increase of about 28% for the wet gas scenario under SG3. On the other hand, dry gas under SG3 leads to a maximum increase of about 9%, and under SG2 still displays a percent decrease in SOMO35 that covers most of the British basin region (a maximum percent decrease in SOMO35 of circa –7%). These findings underline the important role of VOC emissions in increasing O_3 production and in turn worsening adverse health effects, and that effects are primarily localized to the countries where shale gas is being produced and the closely surrounding region.

Summary and conclusions

Our study offers the opportunity to understand and quantify potential implications from a future European shale gas industry on O_3 air quality. Here we use the WRF-Chem online-coupled regional chemistry transport model where our setup is based on Mar et al. (2016). We explore a total of nine comprehensive emission scenarios which are based on in-depth European shale gas scenarios from Cremonese et al. (2019), and which examine the effects of gas speciation, concentration of NO_x emissions over space and time, and a range of three CH_4 leakage rates on model O_3. Additionally, it is important to emphasize that our results depend on our scenario assumptions; because European shale gas does not yet exist as an industry, the results are not a predictor of what will happen in the future but rather a range of potential impacts, and further the results highlight what may be important for regulation if this industry were to come into existence.

Our results show that shale gas emissions are capable of significantly increasing O_3 concentrations (maximum of 28.4 $\mu g\ m^{-3}$ over the North Sea and maximum of about 22 $\mu g\ m^{-3}$ over land in the UK). Shale gas activities result in up to one third of all valid measurement stations in France and the UK having additional exceedances above the WHO threshold, up to about a fifth of stations in Germany, and a considerable percentage of measurement stations in neighboring and distant countries. Furthermore we find that values of SOMO35, an indicator of health impacts, can be considerable with a maximum percent increase of ~28%, which would further burden O_3-related health issues in Europe (Bell et al., 2014). This also poses concern for a future European shale gas industry where an ageing population is at greater risk to O_3-related health effects (Amann et al., 2008).

The overarching trend found in our results is that VOC emissions are critical to O_3 formation. Impacts were greatest for a scenario in which the VOC emissions are based on the assumptions that shale gas is wet and CH_4 leakage is relatively extreme. While in practice these assumptions together may be unlikely, high VOC emissions are also possible through greater shale gas production, wet gas with an even greater VOC component, and even higher gas leakage. Additionally the findings here demonstrate that concentrated NO_x emissions increase impacts on O_3. However these impacts from concentrating NO_x emissions are relatively low in comparison to impacts from increasing VOC emissions, and become less important as VOC emissions increase.

This study shows a clear potential for a future shale gas industry in Europe to adversely impact local and regional O_3 concentrations and to exacerbate already existing air quality issues in this region. Even in lower VOC emission scenarios, emissions are sufficiently high to effect a considerable number (minimum of 103 when applying the WHO threshold) of additional exceedances. Altogether these results show that future shale gas industries in Germany and the UK pose a threat to European O_3 air quality, and emission control strategies, especially for VOCs and to a lesser extent NO_x, are critical to mitigate impacts. While it is not possible to control the speciation of gas extracted, concerted effort would be required to reduce CH_4 leakage from gas production, and in turn associated VOC emissions. This would offer a three-pronged benefit by reducing detrimental outcomes for air quality, mitigating climate change, and improving the economics since less leakage means that more gas can be brought to market.

Data Accessibility Statement

All model results used in this study are available here:

Weger, Lindsey; Lupascu, Aurelia; Cremonese, Lorenzo; Butler, Tim (2019), Modeling the impact of a potential shale gas industry in Germany and the United Kingdom on ozone with WRF-Chem, v11, Dryad, Dataset, https://doi.org/10.5061/dryad.08kprr4xv

Notes

[1] (Technically recoverable) resources is the volume of gas that can be produced based on current technology. EIA. 2019. Oil and natural gas resource categories reflect varying degrees of certainty. Available at https://www.eia.gov/todayinenergy/detail.php?id=17151.

[2] Gas-in-place refers to the total amount of gas estimated in the reservoir, and not the amount that can be recovered. BGS. 2013. The Carboniferous Bowland Shale gas study: geology and resource estimation.

London, UK: British Geological Survey for Department of Energy and Climate Change.

[3] CH_4 leakage is expressed as total CH_4 emissions divided by total CH_4 (natural gas) produced, for the segment of the natural gas chain under study.

[4] Note that O_3 values are typically reported in units of parts per billion (ppb) for the US while in $\mu g\ m^{-3}$ for the EU, where 1 ppb O_3 is equal to 2.00 $\mu g\ m^{-3}$ at standard temperature and pressure (20°C and 1013.25 mbar). Due to the European focus of this study we will henceforth present our findings in $\mu g\ m^{-3}$, and list values from other studies in their original format.

Supplemental file

The supplemental file for this article can be found as follows:

- **Text S1.** Supplemental text. Text S1 includes the namelist used in the WRF-Chem simulations. A detailed description of the conNO_x scenario development is provided. Statistical data on MDA8 enhancement from shale gas scenarios are included. Exceedance data and plots resulting from scenarios applying the EU threshold for O_3 are also included. Additionally a wind rose diagram of the domain is included, as well as a surface plot of SOMO35 for the base case simulation. DOI: https://doi.org/10.1525/elementa.387.s1

Acknowledgements

The authors would like to thank WRF-Chem developers for making the pre-processing tools and model available to the scientific community. We thank TNO for access to the TNO-MACC III emissions inventory. We also thank Kathleen Mar (IASS) for valuable support regarding the evaluation and Mark Lawrence (IASS) for discussions on the project and manuscript. Moreover we thank Alan Jackson for personal discussion related to scenario development. Additionally we acknowledge the Potsdam Institute for Climate Impact Research for use of their high performance computer system where the WRF-Chem simulations were carried out.

Funding information

This project was funded by the German Federal Ministry of Education and Research (BMBF), German Research for Sustainable Development (FONA) and the Ministry for Science, Research and Culture of the Federal State of Brandenburg.

Competing interests

The authors have no competing interests to declare.

Author contributions

- Contributed to conception and design: LW, AL, LC, TB
- Contributed to acquisition of data: LW, AL, LC
- Contributed to analysis and interpretation of data: LW, AL, LC, TB
- Drafted and/or revised the article: LW, AL, LC, TB
- Approved the submitted version for publication: LW, AL, LC, TB

References

AACOG Natural Resources Department. 2013. Development of the Extended June 2006 Photochemical Modeling Episode. San Antonio. Available at https://www.aacog.com/DocumentCenter/View/19262.

AACOG Natural Resources Department. 2015. Ozone Analysis June 2006 Photochemical Modeling Episode. San Antonio. Available at http://www.aacog.com/DocumentCenter/View/31682.

ACATECH. 2016. Hydraulic Fracturing. A technology under debate (acatech POSITION PAPER). Munich: acatech National Acedemy of Science and Engineering.

Ahmadov, R, McKeen, S, Trainer, M, Banta, R, Brewer, A, Brown, S, Edwards, PM, de Gouw, JA, Frost, GJ, Gilman, J, Helmig, D, Johnson, B, Karion, A, Koss, A, Langford, A, Lerner, B, Olson, J, Oltmans, S, Peischl, J, Pétron, G, Pichugina, Y, Roberts, JM, Ryerson, T, Schnell, R, Senff, C, Sweeney, C, Thompson, C, Veres, PR, Warneke, C, Wild, R, Williams, EJ, Yuan, B and **Zamora, R.** 2015. Understanding high wintertime ozone pollution events in an oil- and natural gas-producing region of the western US. *Atmos Chem Phys* **15**(1): 411–429. DOI: https://doi.org/10.5194/acp-15-411-2015

Allen, DT, Torres, VM, Thomas, J, Sullivan, DW, Harrison, M, Hendler, A, Herndon, SC, Kolb, CE, Fraser, MP, Hill, AD, Lamb, BK, Miskimins, J, Sawyer, RF and **Seinfeld, JH.** 2013. Measurements of methane emissions at natural gas production sites in the United States. *P Natl Acad Sci USA* **110**(44): 17768–17773. DOI: https://doi.org/10.1073/pnas.1304880110

Althaus, M. 2014. Gasland Germany: state of play. *International Shale Gas and Oil Journal* **2**(1).

Alvarez, RA, Pacala, SW, Winebrake, JJ, Chameides, WL and **Hamburg, SP.** 2012. Greater focus needed on methane leakage from natural gas infrastructure. *P Natl Acad Sci USA* **109**(17): 6435–6440. DOI: https://doi.org/10.1073/pnas.1202407109

Alvarez, RA, Zavala-Araiza, D, Lyon, DR, Allen, DT, Barkley, ZR, Brandt, AR, Davis, KJ, Herndon, SC, Jacob, DJ, Karion, A, Kort, EA, Lamb, BK, Lauvaux, T, Maasakkers, JD, Marchese, AJ, Omara, M, Pacala, SW, Peischl, J, Robinson, AL, Shepson, PB, Sweeney, C, Townsend-Small, A, Wofsy, SC and **Hamburg, SP.** 2018. Assessment of methane emissions from the U.S. oil and gas supply chain. *Science* **361**(6398): 186–188. DOI: https://doi.org/10.1126/science.aar7204

Amann, M, Derwent, D, Forsberg, B, Hänninen, O, Hurley, F, Krzyzanowski, M, de Leeuw, F, Liu, SJ, Mandin, C, Schneider, J, Schwarze, P and **Simpson, D.** 2008. Health risks of ozone from long-range transboundary air pollution. Copenhagen, Denmark: World Health Organization Regional Office for Europe. Available at http://www.euro.who.int/en/publications/abstracts/health-risks-of-ozone-from-long-range-transboundary-air-pollution.

AQEG. 2018. Potential Air Quality Impacts of Shale Gas Extraction in the UK. London, UK: Air Quality Expert Group (AQEG).

Archibald, AT, Ordóñez, C, Brent, E and **Williams, ML.** 2018. Potential impacts of emissions associated with unconventional hydrocarbon extraction on UK air quality and human health. *Air Qual Atmos Hlth* **11**(6): 627–637. DOI: https://doi.org/10.1007/s11869-018-0570-8

Atkinson, R. 2000. Atmospheric chemistry of VOCs and NO_x. *Atmos Environ* **34**: 2063–2101. DOI: https://doi.org/10.1016/S1352-2310(99)00460-4

Avnery, S, Mauzerall, DL, Liu, J and **Horowitz, LW.** 2011. Global crop yield reductions due to surface ozone exposure: 1. Year 2000 crop production losses and economic damage. *Atmos Environ* **45**(13): 2284–2296. DOI: https://doi.org/10.1016/j.atmosenv.2010.11.045

Bach, H, Brandt, J, Christensen, JH, Ellermann, T, Geels, C, Hertel, O, Massling, A, Nielsen, HØ, Nielsen, OK, Nordstrøm, C, Nøjgaard, JK, Skov, H, Chatterton, T, Hayes, E, Barnes, J, Laxen, D, Irwin, J, Longhurst, J, Pelsy, F and **Zamparutti, T.** 2014. Services to assess the reasons for non-compliance of ozone target value set by Directive 2008/50/EC and potential for air quality improvements in relation to ozone pollution. Final report. Rotterdam, Netherlands: ECORYS Nederland BV, 1–47.

Baker, RW and **Lokhandwala, K.** 2008. Natural Gas Processing with Membranes: An Overview. *Ind Eng Chem Res* **47**(7): 2109–2121. DOI: https://doi.org/10.1021/ie071083w

Bell, ML, Zanobetti, A and **Dominici, F.** 2014. Who is more affected by ozone pollution? A systematic review and meta-analysis. *Am J Epidemiol* **180**(1): 15–28. DOI: https://doi.org/10.1093/aje/kwu115

BGR. 2012. Abschätzung des Erdgaspotenzials aus dichten Tongesteinen (Schiefergas) in Deutschland. Hannover: Bundesanstalt für Geowissenschaften (BGR).

BGR. 2016. Schieferöl und Schiefergas in Deutschland – Potenziale und Umweltsaspekte. Hannover: Bundesanstalt für Geowissenschaften und Rohstoffe (BGR): 1–197.

BGS. 2013. The Carboniferous Bowland Shale gas study: geology and resource estimation. London, UK: British Geological Survey for Department of Energy and Climate Change.

BP. 2016. BP Energy Outlook 2016 edition. Outlook to 2035. London, UK: BP. Available at https://www.bp.com/energyoutlook.

BP. 2017. BP Energy Outlook 2017 edition. London, UK: BP. Available at https://www.bp.com/energyoutlook.

Brandt, AR, Heath, GA, Kort, EA, O'Sullivan, F, Pétron, G, Jordaan, SM, Tans, P, Wilcox, J, Gopstein, AM, Arent, D, Wofsy, S, Brown, NJ, Bradley, R, Stucky, GD, Eardley, D and **Harriss, R.** 2014. Methane leaks from North American natural gas systems. *Science* **343**(6172): 733–735. DOI: https://doi.org/10.1126/science.1247045

Broomfield, M, Donovan, B and **Leonard, A.** 2014. Considerations for quantifying fugitive methane releases from shale gas operations. Bristol, UK: Environment Agency.

Brunner, D, Savage, N, Jorba, O, Eder, B, Giordano, L, Badia, A, Balzarini, A, Baró, R, Bianconi, R, Chemel, C, Curci, G, Forkel, R, Jiménez-Guerrero, P, Hirtl, M, Hodzic, A, Honzak, L, Im, U, Knote, C, Makar, P, Manders-Groot, A, van Meijgaard, E, Neal, L, Pérez, JL, Pirovano, G, San Jose, R, Schröder, W, Sokhi, RS, Syrakov, D, Torian, A, Tuccella, P, Werhahn, J, Wolke, R, Yahya, K, Zabkar, R, Zhang, Y, Hogrefe, C and **Galmarini, S.** 2015. Comparative analysis of meteorological performance of coupled chemistry-meteorology models in the context of AQMEII phase 2. *Atmos Environ* **115**: 470–498. DOI: https://doi.org/10.1016/j.atmosenv.2014.12.032

Carter, WPL and **Seinfeld, JH.** 2012. Winter ozone formation and VOC incremental reactivities in the Upper Green River Basin of Wyoming. *Atmos Environ* **50**: 255–266. DOI: https://doi.org/10.1016/j.atmosenv.2011.12.025

Caulton, DR, Shepson, PB, Santoro, RL, Sparks, JP, Howarth, RW, Ingraffea, AR, Cambaliza, MOL, Sweeney, C, Karion, A, Davis, KJ, Stirm, BH, Montzka, SA and **Miller, BR.** 2014. Toward a better understanding and quantification of methane emissions from shale gas development. *P Natl Acad Sci USA* **111**(17): 6237–6242. DOI: https://doi.org/10.1073/pnas.1316546111

Chang, C-Y, Faust, E, Hou, X, Lee, P, Kim, HC, Hedquist, BC and **Liao, KJ.** 2016. Investigating ambient ozone formation regimes in neighboring cities of shale plays in the Northeast United States using photochemical modeling and satellite retrievals. *Atmos Environ* **142**: 152–170. DOI: https://doi.org/10.1016/j.atmosenv.2016.06.058

Chen, F and **Dudhia, J.** 2001. Coupling an Advanced Land Surface–Hydrology Model with the Penn State–NCAR MM5 Modeling System. Part I: Model Implementation and Sensitivity. *Mon Weather Rev* **129**: 569–585. DOI: https://doi.org/10.1175/1520-0493(2001)129<0569:CAALSH>2.0.CO;2

Chou, M-D and **Suarez, MJ.** 1994. An efficient thermal infrared radiation parameterization for use in general circulation models. Greenbelt, MD, US: NASA Goddard Space Flight Center, 1–84. Available at https://ntrs.nasa.gov/search.jsp?R=19950009331.

Cotton, M, Rattle, I and **Van Alstine, J.** 2014. Shale gas policy in the United Kingdom: An argumentative discourse analysis. *Energ Policy* **73**: 427–438. DOI: https://doi.org/10.1016/j.enpol.2014.05.031

Cremonese, L, Ferrari, M, Flynn, MP and **Gusev, A.** 2015. Shale Gas and Fracking in Europe. Potsdam: IASS.

Cremonese, L, Weger, LB, Denier van der Gon, HAC, Bartels, M and **Butler, TM.** 2019. Emission scenarios of a potential shale gas industry in Germany and

the United Kingdom. *Elem Sci Anth* **7**(1): 18. DOI: https://doi.org/10.1525/elementa.359

DECC. 2013. Potential Greenhouse Gas Emissions Associated with Shale Gas Extraction and Use. London, UK: Department of Energy and Climate Change (DECC).

DECC. 2014. Fracking UK shale: local air quality. London, UK: Department of Energy and Climate Change (DECC).

Dee, DP, Uppala, SM, Simmons, AJ, Berrisford, P, Poli, P, Kobayashi, S, Andrae, U, Balmaseda, MA, Balsamo, G, Bauer, P, Bechtold, P, Beljaars, ACM, van de Berg, L, Bidlot, J, Bormann, N, Delsol, C, Dragani, R, Fuentes, M, Geer, AJ, Haimberger, L, Healy, SB, Hersbach, H, Hólm, EV, Isaksen, L, Kållberg, P, Köhler, M, Matricardi, M, McNally, AP, Monge-Sanz, BM, Morcrette, JJ, Park, BK, Peubey, C, de Rosnay, P, Tavolato, C, Thépaut, JN and **Vitart, F.** 2011. The ERA-Interim reanalysis: configuration and performance of the data assimilation system. *Q J R Meteorol Soc* **137**: 553–597. DOI: https://doi.org/10.1002/qj.828

EC. 2014. Exploration and production of hydrocarbons (such as shale gas) using high volume hydraulic fracturing in the EU. Brussels: European Commission.

Edwards, PM, Brown, SS, Roberts, JM, Ahmadov, R, Banta, RM, de Gouw, JA, Dubé, WP, Field, RA, Flynn, JH, Gilman, JB, Graus, M, Helmig, D, Koss, A, Langford, AO, Lefer, BL, Lerner, BM, Li, R, Li, SM, McKeen, SA, Murphy, SM, Parrish, DD, Senff, CJ, Soltis, J, Stutz, J, Sweeney, C, Thompson, CR, Trainer, MK, Tsai, C, Veres, PR, Washenfelder, RA, Warneke, C, Wild, RJ, Young, CJ, Yuan, B and **Zamora, R.** 2014. High winter ozone pollution from carbonyl photolysis in an oil and gas basin. *Nature* **514**: 351. DOI: https://doi.org/10.1038/nature13767

EEA. 2013. AirBase, The European Air Quality Database, version 7 [dataset]. Copenhagen, Denmark: European Environment Agency. Available at http://www.eea.europa.eu/data-and-maps/data/airbase-the-european-air-quality-database-7. Accessed September 22, 2017.

EEA. 2014. Air quality in Europe — 2014 report. Copenhagen, Denmark: European Environment Agency. No 5/2014. Available at https://www.eea.europa.eu/publications/air-quality-in-europe-2014.

EEA. 2017. Air quality in Europe — 2017 report. Copenhagen, Denmark: European Environment Agency. No 13/2017. Available at https://www.eea.europa.eu/publications/air-quality-in-europe-2017.

EIA. 2013. Technically Recoverable Shale Oil and Shale Gas Resources: An Assessment of 137 Shale Formations in 41 Countries Outside the United States. Washington, DC, US: US Energy Information Administration (EIA).

EIA. 2016. Annual energy outlook 2016 with projections to 2040. Washington, DC, US: US Energy Information Administration (EIA).

EIA. 2018. Frequently asked questions. How much shale gas is produced in the United States? Available at https://www.eia.gov/tools/faqs/faq.php?id=907&t=8. Accessed September 6, 2019.

EIA. 2019a. Natural Gas. Available at https://www.eia.gov/dnav/ng/hist/n9070us2A.htm. Accessed March 15, 2019.

EIA. 2019b. Oil and natural gas resource categories reflect varying degrees of certainty. Available at https://www.eia.gov/todayinenergy/detail.php?id=17151.

Emmons, LK, Walters, S, Hess, PG, Lamarque, J-F, Pfister, GG, Fillmore, D, Granier, C, Guenther, A, Kinnison, D, Laepple, T, Orlando, J, Tie, X, Tyndall, G, Wiedinmyer, C, Baughcum, SL and **Kloster, S.** 2010. Description and evaluation of the Model for Ozone and Related chemical Tracers, version 4 (MOZART-4). *Geosci Model Dev* **3**(1): 43–67. DOI: https://doi.org/10.5194/gmd-3-43-2010

EP. 2002. Directive 2002/3/EC of the European Parliament and of the council of 12 February 2002 relating to ozone in ambient air. in: European Parliament, ed. Brussels, Belgium: OJ.

EPA. 2013. Integrated science assessment for ozone and related photochemical oxidants. Research Triangle Park, NC, US: U.S. Environmental Protection Agency.

Fallmann, J, Forkel, R and **Emeis, S.** 2016. Secondary effects of urban heat island mitigation measures on air quality. *Atmos Environ* **125**: 199–211. DOI: https://doi.org/10.1016/j.atmosenv.2015.10.094

Fann, N, Baker, KR, Chan, EAW, Eyth, A, Macpherson, A, Miller, E and **Snyder, J.** 2018. Assessing Human Health PM 2.5 and Ozone Impacts from U.S. Oil and Natural Gas Sector Emissions in 2025. *Environ Sci Technol* **52**(15): 8095–8103. DOI: https://doi.org/10.1021/acs.est.8b02050

Faramawy, S, Zaki, T and **Sakr, AAE.** 2016. Natural gas origin, composition, and processing: A review. *J Nat Gas Sci Eng* **34**: 34–54. DOI: https://doi.org/10.1016/j.jngse.2016.06.030

Fast, JD, Gustafson, WI, Easter, RC, Zaveri, RA, Barnard, JC, Chapman, EG, Grell, GA and **Peckham, SE.** 2006. Evolution of ozone, particulates, and aerosol direct radiative forcing in the vicinity of Houston using a fully coupled meteorology-chemistry-aerosol model. *J Geophys Res-Atmos* **111**(D21). DOI: https://doi.org/10.1029/2005JD006721

Field, RA, Soltis, J, McCarthy, MC, Murphy, S and **Montague, DC.** 2015. Influence of oil and gas field operations on spatial and temporal distributions of atmospheric non-methane hydrocarbons and their effect on ozone formation in winter. *Atmos Chem Phys* **15**(6): 3527–3542. DOI: https://doi.org/10.5194/acp-15-3527-2015

Forkel, R, Werhahn, J, Hansen, AB, McKeen, S, Peckham, S, Grell, G and **Suppan, P.** 2012. Effect of aerosol-radiation feedback on regional air quality – A case study with WRF/Chem. *Atmos Environ* **53**: 202–211. DOI: https://doi.org/10.1016/j.atmosenv.2011.10.009

Gavidia-Calderón, M, Vara-Vela, A, Crespo, NM and **Andrade, MF.** 2018. Impact of time-dependent chemical boundary conditions on tropospheric ozone simulation with WRF-Chem: An experiment over the Metropolitan Area of São Paulo. *Atmos Environ* **195**: 112–124. DOI: https://doi.org/10.1016/j.atmosenv.2018.09.026

German Federal Government. 2017. Package of regulations comes into force – No fracking in Germany. Available at https://www.bundesregierung.de/breg-en/issues/sustainability/no-fracking-in-germany-391340. Accessed November 5, 2018.

Gilman, JB, Lerner, BM, Kuster, WC and **de Gouw, JA.** 2013. Source Signature of Volatile Organic Compounds from Oil and Natural Gas Operations in Northeastern Colorado. *Environ Sci Technol* **47**(3): 1297–1305. DOI: https://doi.org/10.1021/es304119a

Grell, GA and **Dévényi, D.** 2002. A generalized approach to parameterizing convection combining ensemble and data assimilation techniques. *Geophys Res Lett* **29**(14): 38-1-38-4. DOI: https://doi.org/10.1029/2002GL015311

Grell, GA, Knoche, R, Peckham, SE and **McKeen, SA.** 2004. Online versus offline air quality modeling on cloud-resolving scales. *Geophys Res Lett* **31**(16). DOI: https://doi.org/10.1029/2004GL020175

Grell, GA, Peckham, SE, Schmitz, R, McKeen, SA, Frost, G, Skamarock, WC and **Eder, B.** 2005. Fully coupled "online" chemistry within the WRF model. *Atmos Environ* **39**: 6957–6975. DOI: https://doi.org/10.1016/j.atmosenv.2005.04.027

Hays, J, Finkel, ML, Depledge, M, Law, A and **Shonkoff, SBC.** 2015. Considerations for the development of shale gas in the United Kingdom. *Sci Total Environ* **512–513**: 36–42. DOI: https://doi.org/10.1016/j.scitotenv.2015.01.004

Helmig, D, Thompson, CR, Evans, J, Boylan, P, Hueber, J and **Park, JH.** 2014. Highly Elevated Atmospheric Levels of Volatile Organic Compounds in the Uintah Basin, Utah. *Environ Sci Technol* **48**(9): 4707–4715. DOI: https://doi.org/10.1021/es405046r

Hong, S-Y, Noh, Y and **Dudhia, J.** 2006. A new vertical diffusion package with an explicit treatment of entrainment processes. *Mon Weather Rev* **134**: 2318–2341. DOI: https://doi.org/10.1175/MWR3199.1

Horvath, SM and **McKee, DJ.** 1993. Chapter 3, Acute and chronic health effects of ozone. In: *Tropospheric Ozone: Human Health and Agricultural Impacts*. 1st ed., 39–84. Boca Raton, Florida, US: CRC Press.

Howarth, RW. 2014. A bridge to nowhere: methane emissions and the greenhouse gas footprint of natural gas. *Energy Sci Eng* **2**(2): 47–60. DOI: https://doi.org/10.1002/ese3.35

HTAP. 2010. Hemispheric transport of air pollution 2010. Part A: ozone and particulate matter. Geneva, Switzerland: Task Force on Hemispheric Transport of Air Pollution (HTAP).

Iacono, MJ, Delamere, JS, Mlawer, EJ, Shephard, MW, Clough, SA and **Collins, WD.** 2008. Radiative forcing by long-lived greenhouse gases: Calculations with the AER radiative transfer models. *J Geophys Res-Atmos* **113**(D13). DOI: https://doi.org/10.1029/2008JD009944

Im, U, Bianconi, R, Solazzo, E, Kioutsioukis, I, Badia, A, Balzarini, A, Baró, R, Bellasio, R, Brunner, D, Chemel, C, Curci, G, Flemming, J, Forkel, R, Giordano, L, Jiménez-Guerrero, P, Hirtl, M, Hodzic, A, Honzak, L, Jorba, O, Knote, C, Kuenen, JJP, Makar, PA, Manders-Groot, A, Neal, L, Pérez, JL, Pirovano, G, Pouliot, G, San, Jose, R, Savage, N, Schroder, W, Sokhi, RS, Syrakov, D, Torian, A, Tuccella, P, Werhahn, J, Wolke, R, Yahya, K, Zabkar, R, Zhang, Y, Zhang, J, Hogrefe, C and **Galmarini, S.** 2015. Evaluation of operational online-coupled regional air quality models over Europe and North America in the context of AQMEII phase 2. Part I: Ozone. *Atmos Environ* **115**: 404–420. DOI: https://doi.org/10.1016/j.atmosenv.2014.09.042

Jiménez, PA, Dudhia, J, González-Rouco, JF, Navarro, J, Montávez, JP and **García-Bustamante, E.** 2012. A revised scheme for the WRF surface layer formulation. *Mon Weather Rev* **140**: 898–918. DOI: https://doi.org/10.1175/MWR-D-11-00056.1

Johnson, MR, Tyner, DR, Conley, S, Schwietzke, S and **Zavala-Araiza, D.** 2017. Comparisons of Airborne Measurements and Inventory Estimates of Methane Emissions in the Alberta Upstream Oil and Gas Sector. *Environ Sci Technol* **51**(21): 13008–13017. DOI: https://doi.org/10.1021/acs.est.7b03525

JRC. 2012. Unconventional Gas: Potential Energy Market Impacts in the European Union. Luxembourg: Joint Research Centre Institute for Energy and Transport.

Karion, A, Sweeney, C, Pétron, G, Frost, G, Michael, Hardesty, R, Kofler, J, Miller, BR, Newberger, T, Wolter, S, Banta, R, Brewer, A, Dlugokencky, E, Lang, P, Montzka, SA, Schnell, R, Tans, P, Trainer, M, Zamora, R and **Conley, S.** 2013. Methane emissions estimate from airborne measurements over a western United States natural gas field. *Geophys Res Lett* **40**(16): 4393–4397. DOI: https://doi.org/10.1002/grl.50811

Karlický, J, Huszár, P and **Halenka, T.** 2017. Validation of gas phase chemistry in the WRF-Chem model over Europe. *Adv Sci Res* **14**: 181–186. DOI: https://doi.org/10.5194/asr-14-181-2017

Kemball-Cook, S, Bar-Ilan, A, Grant, J, Parker, L, Jung, J, Santamaria, W, Mathews, J and **Yarwood, G.** 2010. Ozone impacts of natural gas development in the Haynesville Shale. *Environ Sci Technol* **44**(24): 9357–9363. DOI: https://doi.org/10.1021/es1021137

Koss, AR, de Gouw, J, Warneke, C, Gilman, JB, Lerner, BM, Graus, M, Yuan, B, Edwards, P, Brown, SS, Wild, R, Roberts, JM, Bates, TS and **Quinn, PK.** 2015. Photochemical aging of volatile organic compounds associated with oil and natural gas

extraction in the Uintah Basin, UT, during a wintertime ozone formation event. *Atmos Chem Phys* **15**(10): 5727–5741. DOI: https://doi.org/10.5194/acp-15-5727-2015

Kuenen, JJP, Visschedijk, AJH, Jozwicka, M and **Denier van der Gon, HAC.** 2014. TNO-MACC_II emission inventory; a multi-year (2003–2009) consistent high-resolution European emission inventory for air quality modelling. *Atmos Chem Phys* **14**(20). DOI: https://doi.org/10.5194/acp-14-10963-2014

Kuik, F, Kerschbaumer, A, Lauer, A, Lupascu, A, von Schneidemesser, E and **Butler, TM.** 2018. Top–down quantification of NO_x emissions from traffic in an urban area using a high-resolution regional atmospheric chemistry model. *Atmos Chem Phys* **18**(11): 8203–8225. DOI: https://doi.org/10.5194/acp-18-8203-2018

Kuik, F, Lauer, A, Churkina, G, Denier van der Gon, HAC, Fenner, D, Mar, KA and **Butler, TM.** 2016. Air quality modelling in the Berlin–Brandenburg region using WRF-Chem v3.7.1: sensitivity to resolution of model grid and input data. *Geosci Model Dev* **9**(12): 4339–4363. DOI: https://doi.org/10.5194/gmd-9-4339-2016

Kumar, P and **Imam, B.** 2013. Footprints of air pollution and changing environment on the sustainability of built infrastructure. *Sci Total Environ* **444**: 85–101. DOI: https://doi.org/10.1016/j.scitotenv.2012.11.056

Kusaka, H and **Kimura, F.** 2004. Thermal effects of urban canyon structure on the nocturnal heat island: Numerical experiment using a mesoscale model coupled with an urban canopy model. *J Appl Meteorol* **43**: 1899–1910. DOI: https://doi.org/10.1175/JAM2169.1

LaBelle, M. 2018. Chapter 4, Disappointed Expectations: Energy Security vs. Bureaucracy and Geology. In: *The Shale Dilemma: A Global Perspective on Fracking and Shale Development*, 178–203. Pittsburgh, Pennsylvania, US: University of Pittsburgh Press.

Lee, DS, Holland, MR and **Falla, N.** 1996. The potential impact of ozone on materials in the U.K. *Atmos Environ* **30**(7): 1053–1065. DOI: https://doi.org/10.1016/1352-2310(95)00407-6

Lin, Y-L, Farley, RD and **Orville, HD.** 1983. Bulk parameterization of the snow field in a cloud model. *J Clim Appl Meteorol* **22**: 1065–1092. DOI: https://doi.org/10.1175/1520-0450(1983)022<1065:BPOTSF>2.0.CO;2

Mar, KA, Ojha, N, Pozzer, A and **Butler, TM.** 2016. Ozone air quality simulations with WRF-Chem (v3.5.1) over Europe: model evaluation and chemical mechanism comparison. *Geosci Model Dev* **9**(10): 3699–3728. DOI: https://doi.org/10.5194/gmd-9-3699-2016

McGlade, C, Bradshaw, M, Anandarajah, G, Watson, J and **Ekins, P.** 2014. A Bridge to a Low-Carbon Future? Modelling the Long-Term Global Potential of Natural Gas – Research Report. London: UK Energy Research Centre (UKERC).

Met Office. 2006. MIDAS: Global Weather Observation Data. NCAS British Atmospheric Data Centre [dataset]. Oxford, UK: Centre for Environmental Data Analysis. Available at http://catalogue.ceda.ac.uk/uuid/0ec59f09b3158829a059fe70b17de951. Accessed June 23, 2017.

Miguez-Macho, G, Stenchikov, GL and **Robock, A.** 2004. Spectral nudging to eliminate the effects of domain position and geometry in regional climate model simulations. *J Geophys Res-Atmos* **109**(D13). DOI: https://doi.org/10.1029/2003JD004495

Miller, SM, Wofsy, SC, Michalak, AM, Kort, EA, Andrews, AE, Biraud, SC, Dlugokencky, EJ, Eluszkiewicz, J, Fischer, ML, Janssens-Maenhout, G, Miller, BR, Miller, JB, Montzka, SA, Nehrkorn, T and **Sweeney, C.** 2013. Anthropogenic emissions of methane in the United States. *P Natl Acad Sci USA* **110**(50): 20018–20022. DOI: https://doi.org/10.1073/pnas.1314392110

Monks, PS, Archibald, AT, Colette, A, Cooper, O, Coyle, M, Derwent, R, Fowler, D, Granier, C, Law, KS, Mills, GE, Stevenson, DS, Tarasova, O, Thouret, V, von Schneidemesser, E, Sommariva, R, Wild, O and **Williams, ML.** 2015. Tropospheric ozone and its precursors from the urban to the global scale from air quality to short-lived climate forcer. *Atmos Chem Phys* **15**(15): 8889–8973. DOI: https://doi.org/10.5194/acp-15-8889-2015

MULNV NRW. 2012. Fracking in unkonventionellen Erdgas-Lagerstätten in NRW. Düsseldorf: Ministerium für Klimaschutz, Umwelt, Landwirtschaft, Natur- und Verbraucherschutz des Landes Nordrhein-Westfalen (MULNV NRW).

Myhre, G, Shindell, D, Bréon, F-M, Collins, W, Fuglestvedt, J, Huang, J, Koch, D, Lamarque, JF, Lee, D, Mendoza, B, Nakajima, T, Robock, A, Stephens, G, Takemura, T and **Zhang, H.** 2013. Anthropogenic and Natural Radiative Forcing. In: *Climate Change 2013: The Physical Science Basis. Contribution of Working Group I to the Fifth Assessment Report of the Intergovernmental Panel on Climate Change*. Cambridge, United Kingdom and New York, NY, USA.

NC Division of Air Quality. 2015. Photochemical Modeling of Shale Gas Development and Production in North Carolina. NC Division of Air Quality.

Nuvolone, D, Petri, D and **Voller, F.** 2018. The effects of ozone on human health. *Environ Sci Pollut Res* **25**(9): 8074–8088. DOI: https://doi.org/10.1007/s11356-017-9239-3

Olaguer, EP. 2012. The potential near-source ozone impacts of upstream oil and gas industry emissions. *J Air Waste Manage Assoc* **62**(8): 966–977. DOI: https://doi.org/10.1080/10962247.2012.688923

Peischl, J, Ryerson, TB, Aikin, KC, de Gouw, JA, Gilman, JB, Holloway, JS, Lerner, BM, Nadkarni, R, Neuman, JA, Nowak, JB, Trainer, M, Warneke, C and **Parrish, DD.** 2015. Quantifying atmospheric methane emissions from the

Haynesville, Fayetteville, and northeastern Marcellus shale gas production regions. *J Geophys Res-Atmos* **120**(5): 2119–2139. DOI: https://doi.org/10.1002/2014JD022697

Peischl, J, Ryerson, TB, Brioude, J, Aikin, KC, Andrews, AE, Atlas, E, Blake, D, Daube, BC, de Gouw, JA, Dlugokencky, E, Frost, GJ, Gentner, DR, Gilman, JB, Goldstein, AH, Harley, RA, Holloway, JS, Kofler, J, Kuster, WC, Lang, PM, Novelli, PC, Santoni, GW, Trainer, M, Wofsy, SC and **Parrish, DD.** 2013. Quantifying sources of methane using light alkanes in the Los Angeles basin, California. *J Geophys Res-Atmos* **118**(10): 4974–4990. DOI: https://doi.org/10.1002/jgrd.50413

Perry, C. 2018. Re: Department for Business Energy & Industrial Strategy hydraulic fraturing consent. In: Department for Business Energy & Industrial Strategy, ed. London, UK.

Pétron, G, Frost, G, Miller, BR, Hirsch, AI, Montzka, SA, Karion, A, Trainer, M, Sweeney, C, Andrews, AE, Miller, L, Kofler, J, Bar-Ilan, A, Dlugokencky, EJ, Patrick, L, Moore, CT, Ryerson, TB, Siso, C, Kolodzey, W, Lang, PM, Conway, T, Novelli, Paul, Masarie, K, Hall, B, Guenther, D, Kitzis, D, Miller, J, Welsh, D, Wolfe, D, Neff, W and **Tans, P.** 2012. Hydrocarbon emissions characterization in the Colorado Front Range: A pilot study. *J Geophys Res-Atmos* **117**(D4). DOI: https://doi.org/10.1029/2011JD016360

Pétron, G, Karion, A, Sweeney, C, Miller, BR, Montzka, SA, Frost, GJ, Trainer, M, Tans, P, Andrews, A, Kofler, J, Helmig, D, Guenther, D, Dlugokencky, E, Lang, P, Newberger, T, Wolter, S, Hall, B, Novelli, P, Brewer, A, Conley, S, Hardesty, M, Banta, R, White, A, Noone, D, Wolfe, D and **Schnell, R.** 2014. A new look at methane and nonmethane hydrocarbon emissions from oil and natural gas operations in the Colorado Denver-Julesburg Basin. *J Geophys Res-Atmos* **119**(11): 6836–6852. DOI: https://doi.org/10.1002/2013JD021272

Pfister, GG, Parrish, DD, Worden, H, Emmons, LK, Edwards, DP, Wiedinmyer, C, Diskin, GS, Huey, G, Oltmans, SJ, Thouret, V, Weinheimer, A and **Wisthaler, A.** 2011. Characterizing summertime chemical boundary conditions for airmasses entering the US West Coast. *Atmos Chem Phys* **11**(4): 1769–1790. DOI: https://doi.org/10.5194/acp-11-1769-2011

Pfunt, H. 2016. Numerical modeling of fracking fluid migration through fault zones and fractures in the North German Basin. *Hydrogeol J* **24**(6): 1343–1358. DOI: https://doi.org/10.1007/s10040-016-1418-7

Riddick, SN, Mauzerall, DL, Celia, M, Harris, NRP, Allen, G, Pitt, J, Staunton-Sykes, J, Forster, GL, Kang, M, Lowry, D, Nisbet, EG and **Manning, AJ.** 2019. Measuring methane emissions from oil and gas platforms in the North Sea. *Atmos Chem Phys* **19**(15): 9787–9796. DOI: https://doi.org/10.5194/acp-2019-90

Rodriguez, M, Barna, M and **Moore, T.** 2009. Regional impacts of oil and gas development on ozone formation in the western United States. *J Air Waste Manage Assoc* **59**(9): 1111–1118. DOI: https://doi.org/10.3155/1047-3289.59.9.1111

Roy, AA, Adams, PJ and **Robinson, AL.** 2014. Air pollutant emissions from the development, production, and processing of Marcellus Shale natural gas. *J Air Waste Manage Assoc* **64**(1): 19–37. DOI: https://doi.org/10.1080/10962247.2013.826151

Russell, A and **Dennis, R.** 2000. NARSTO critical review of photochemical models and modeling. *Atmos Environ* **34**(12): 2283–2324. DOI: https://doi.org/10.1016/S1352-2310(99)00468-9

Saunois, M, Bousquet, P, Poulter, B, Peregon, A, Ciais, P, Canadell, JG, Dlugokencky, EJ, Etiope, G, Bastviken, D, Houweling, S, Janssens-Maenhout, G, Tubiello, FN, Castaldi, S, Jackson, RB, Alexe, M, Arora, VK, Beerling, DJ, Bergamaschi, P, Blake, DR, Brailsford, G, Brovkin, V, Bruhwiler, L, Crevoisier, C, Crill, P, Covey, K, Curry, C, Frankenberg, C, Gedney, N, Höglund-Isaksson, L, Ishizawa, M, Ito, A, Joos, F, Kim, H, Kleinen T, Krummel, P, Lamarque, J, Langenfelds, R, Locatelli, R, Machida, T, Maksyutov, S, McDonald, KC, Marshall, J, Melton, JR, Morino, I, Naik, V, O'Doherty, S, Parmentier, F, Patra, PK, Peng, C, Peng, S, Peters, GP, Pison, I, Prigent, C, Prinn, R, Ramonet, M, Riley, WJ, Saito, M, Santini, M, Schroeder, R, Simpson, IJ, Spahni, R, Steele, P, Takizawa, A, Thornton, BF, Tian, H, Tohjima, Y, Viovy, N, Voulgarakis, A, van Weele, M, van der Werf, GR, Weiss, R, Wiedinmyer, C, Wilton, DJ, Wiltshire, A, Worthy, D, Wunch, D, Xu, X, Yoshida, Y, Zhang, B, Zhang, Z and **Zhu, Q.** 2016. The global methane budget 2000–2012. *Earth Syst Sci Data* **8**(2): 697–751. DOI: https://doi.org/10.5194/essd-8-697-2016

Sauter, M, Schafmeister, M-T, Peiffer, S, Kuntz, D, Schiedek, T and **Himmelsbach, T.** 2013. Fracking – Die Rolle der Hydrogeologie. *Grundwasser* **18**(3): 157–158. DOI: https://doi.org/10.1007/s00767-013-0228-2

Schade, GW. 2017. How has the US fracking boom affected air pollution in shale areas? Available at https://theconversation.com/how-has-the-us-fracking-boom-affected-air-pollution-in-shale-areas-66190. Accessed February 28, 2019.

Schade, GW and **Roest, G.** 2016. Analysis of non-methane hydrocarbon data from a monitoring station affected by oil and gas development in the Eagle Ford shale, Texas. *Elem Sci Anth* **4**: 000096. DOI: https://doi.org/10.12952/journal.elementa.000096

Schneising, O, Burrows, JP, Dickerson, RR, Buchwitz, M, Reuter, M and **Bovensmann, H.** 2014. Remote sensing of fugitive methane emissions from oil and gas production in North American tight geologic formations. *Earths Future* **2**(10): 548–558. DOI: https://doi.org/10.1002/2014EF000265

Schnell, RC, Oltmans, SJ, Neely, RR, Endres, MS, Molenar, JV and **White, AB.** 2009. Rapid photochemical production of ozone at high concentrations in a rural site during winter. *Nat Geosci* **2**: 120. DOI: https://doi.org/10.1038/ngeo415

SGD. 2013. Stellungnahme zu den geowissenschaftlichen Aussagen des UBA-Gutachtens, der Studie NRW und der Risikostudie des ExxonMobil Info-Dialogprozesses zum Thema Fracking. Hannover: Staatlichen Geologischen Dienste der Deutschen Bundesländer (SGD).

Sillman, S. 1999. The relation between ozone, NO_x and hydrocarbons in urban and polluted rural environments. *Atmos Environ* **33**(12): 1821–1845. DOI: https://doi.org/10.1016/S1352-2310(98)00345-8

Sillman, S. 2003. Chapter 11, Tropospheric Ozone and Photochemical Smog. In: *Environmental Geochemistry* **9**: 407–432. Oxford, UK: Elsevier. DOI: https://doi.org/10.1016/B0-08-043751-6/09053-8

Skamarock, WC, Klemp, JB, Dudhia, J, Gill, DO, Barker, DM, Duda, MG, Huang, XY, Wang, W and **Powers, JG.** 2008. A Description of the Advanced Research WRF Version 3. Boulder, Colorado, US. NCAR/TN–475+STR/NCAR Technical Note.

Society, R. 2012. Shale gas extraction in the UK: a review of hydraulic fracturing. London, UK: The Royal Society.

Solazzo, E, Bianconi, R, Pirovano, G, Matthias, V, Vautard, R, Moran, MD, Wyat, Appel, K, Bessagnet, B, Brandt, J, Christensen, JH, Chemel, C, Coll, I, Ferreira, J, Forkel, R, Francis, XV, Grell, G, Grossi, P, Hansen, AB, Miranda, AI, Nopmongcol, U, Prank, M, Sartelet, KN, Schaap, M, Silver, JD, Sokhi, RS, Vira, J, Werhahn, J, Wolke, R, Yarwood, G, Zhang, J, Rao, ST and **Galmarini, S.** 2012a. Operational model evaluation for particulate matter in Europe and North America in the context of AQMEII. *Atmos Environ* **53**: 75–92. DOI: https://doi.org/10.1016/j.atmosenv.2012.02.045

Solazzo, E, Bianconi, R, Vautard, R, Appel, KW, Moran, MD, Hogrefe, C, Bessagnet, B, Brandt, J, Christensen, JH, Chemel, C, Coll, I, Denier van der, Gon, H, Ferreira, J, Forkel, R, Francis, XV, Grell, G, Grossi, P, Hansen, AB, Jerićević, A, Kraljević, L, Miranda, AI, Nopmongcol, U, Pirovano, G, Prank, M, Riccio, A, Sartelet, KN, Schaap, M, Silver, JD, Sokhi, RS, Vira, J, Werhahn, J, Wolke, R, Yarwood, G, Zhang, J, Rao, ST and **Galmarini, S.** 2012b. Model evaluation and ensemble modelling of surface-level ozone in Europe and North America in the context of AQMEII. *Atmos Environ* **53**: 60–74. DOI: https://doi.org/10.1016/j.atmosenv.2012.01.003

SRU. 2013. Fracking zur Schiefergasgewinnung. Berlin: Sachverständigenrat für Umweltfragen (SRU).

Stamford, L and **Azapagic, A.** 2014. Life cycle environmental impacts of UK shale gas. *Appl Energ* **134**: 506–518. DOI: https://doi.org/10.1016/j.apenergy.2014.08.063

Stegehuis, AI, Vautard, R, Ciais, P, Teuling, AJ, Miralles, DG and **Wild, M.** 2015. An observation-constrained multi-physics WRF ensemble for simulating European mega heat waves. *Geosci Model Dev* **8**(7): 2285–2298. DOI: https://doi.org/10.5194/gmd-8-2285-2015

Stern, R, Builtjes, PJH, Schaap, M, Timmermans, R, Vautard, R, Hodzic, A, Memmesheimer, M, Feldmann, H, Renner, E, Wolke, R and **Kerschbaumer, A.** 2008. A model inter-comparison study focussing on episodes with elevated PM10 concentrations. *Atmos Environ* **42**: 4567–4588. DOI: https://doi.org/10.1016/j.atmosenv.2008.01.068

Stockwell, WR, Kirchner, F, Kuhn, M and **Seefeld, S.** 1997. A new mechanism for regional atmospheric chemistry modeling. *J Geophys Res-Atmos* **102**(D22): 25847–25879. DOI: https://doi.org/10.1029/97JD00849

Thomas, N and **Pickard, J.** 2019. UK fracking struggles to shake off fears of more tremors. Available at https://www.ft.com/content/38fe9eac-c8c4-11e9-a1f4-3669401ba76f. Accessed September 4, 2019.

Tuccella, P, Curci, G, Visconti, G, Bessagnet, B, Menut, L and **Park, RJ.** 2012. Modeling of gas and aerosol with WRF/Chem over Europe: Evaluation and sensitivity study. *J Geophys Res-Atmos* **117**(D3). DOI: https://doi.org/10.1029/2011JD016302

UBA. 2013. Environmental Impacts of Fracking Related to Exploration and Exploitation of Unconventional Natural Gas Deposits. Dessau: Umweltbundesamt (UBA).

UBA. 2014. Umweltauswirkungen von Fracking bei der Aufsuchung und Gewinnung von Erdgasinsbesondere aus Schiefergaslagerstätten. Dessau: Umweltbundesamt (UBA).

Vetter, A. 2016. Shale gas in Germany – the current status. Available at http://www.shale-gas-information-platform.org/areas/the-debate/shale-gas-in-germany-the-current-status.html. Accessed March 3, 2019.

Visschedijk, AJH, Denier van der Gon, HAC, Doornenbal, HC and **Cremonese, L.** 2018. Methane and ethane emission scenarios for potential shale gas production in Europe. *Adv Geosci* **45**: 125–131. DOI: https://doi.org/10.5194/adgeo-45-125-2018

Volz-Thomas, A and **Ridley, BA.** 1994. Chapter 5, Tropospheric Ozone. In: *Scientific Assessment of Ozone Depletion: 1994, Global Ozone Research and Monitoring Project—Report No 37*, 5.1–5.21. Geneva, Switzerland: World Meteorological Organization.

WHO. 2005. WHO Air quality guidelines for particulate matter, ozone, nitrogen dioxide and sulfur dioxide. Global update 2005. Summary of risk assessment. Geneva, Switzerland: World Health Organization.

WHO. 2013. Review of evidence on health aspects of air pollution – REVIHAAP Project Technical Report. Copenhagen, Denmark: WHO Regional Office for Europe.

Yacovitch, TI, Neininger, B, Herndon, SC, Denier van der Gon, HAC, Jonkers, S, Hulskotte, J, Roscioli, JR and **Zavala-Araiza, D.** 2018. Methane emissions in the Netherlands: The Groningen field. *Elem Sci Anth* **6**(57). DOI: https://doi.org/10.1525/elementa.308

Yeo, S. 2019. 'We bloody live here, and it's not fair': How communities in the U.K. are taking on fracking. *Pacific Standard*. Santa Barbara, California, US: PacificStandard.

Zavala-Araiza, D, Lyon, DR, Alvarez, RA, Davis, KJ, Harriss, R, Herndon, SC, Karion, A, Kort, EA, Lamb, BK, Lan, X, Marchese, AJ, Pacala, SW, Robinson, AL, Shepson, PB, Sweeney, C, Talbot, R, Townsend-Small, A, Yacovitch, TI, Zimmerle, DJ and **Hamburg, SP.** 2015. Reconciling divergent estimates of oil and gas methane emissions. *P Natl Acad Sci USA* **112**(51): 15597–15602. DOI: https://doi.org/10.1073/pnas.1522126112

Zaveri, RA and **Peters, LK.** 1999. A new lumped structure photochemical mechanism for large-scale applications. *J Geophys Res-Atmos* **104**(D23): 30387–30415. DOI: https://doi.org/10.1029/1999JD900876

Zhang, Y, Sartelet, K, Wu, S-Y and **Seigneur, C.** 2013a. Application of WRF/Chem-MADRID and WRF/Polyphemus in Europe – Part 1: Model description, evaluation of meteorological predictions, and aerosol–meteorology interactions. *Atmos Chem Phys* **13**(14): 6807–6843. DOI: https://doi.org/10.5194/acp-13-6807-2013

Zhang, Y, Sartelet, K, Zhu, S, Wang, W, Wu, S-Y, Zhang, X, Wang, K, Tran, P, Seigneur, C and **Wang, ZF.** 2013b. Application of WRF/Chem-MADRID and WRF/Polyphemus in Europe – Part 2: Evaluation of chemical concentrations and sensitivity simulations. *Atmos Chem Phys* **13**(14): 6845–6875. DOI: https://doi.org/10.5194/acp-13-6845-2013

How to cite this article: Weger, LB, Lupascu, A, Cremonese, L and Butler, T. 2019. Modeling the impact of a potential shale gas industry in Germany and the United Kingdom on ozone with WRF-Chem. *Elem Sci Anth,* 7: 49. DOI: https://doi.org/10.1525/elementa.387

Domain Editor-in-Chief: Detlev Helmig, Institute of Alpine and Arctic Research, University of Colorado Boulder, US

Guest Editor: Stefan Schwietzke, Environmental Defense Fund, US

Knowledge Domain: Atmospheric Science

Submitted: 13 April 2019 **Accepted:** 09 November 2019 **Published:** 06 December 2019

ELEMENTA Science of the Anthropocene

Elem Sci Anth is a peer-reviewed open access journal published by University of California Press.

OPEN ACCESS